catalysts

MDPI

Review

Perovskites as Catalysts in Advanced Oxidation Processes for Wastewater Treatment

María Luisa Rojas-Cervantes * and Eva Castillejos

Departamento de Química Inorgánica y Química Técnica, Facultad de Ciencias, UNED. Paseo Senda del Rey nº 9, Madrid 28040, Spain; castillejoseva@ccia.uned.es

* Correspondence: mrojas@ccia.uned.es

Received: 1 February 2019; Accepted: 13 February 2019; Published: 2 March 2019

Abstract: Advanced oxidation processes (AOPs), based on the formation of highly reactive radicals are able to degrade many organic contaminants present in effluent water. In the heterogeneous AOPS the presence of a solid which acts as catalyst in combination with other systems (O_3, H_2O_2, light) is required. Among the different materials that can catalyse these processes, perovskites are found to be very promising, because they are highly stable and exhibit a high mobility of network oxygen with the possibility of forming vacancies and to stabilize unusual oxidation states of metals. In this review, we show the fundaments of different kinds of AOPs and the application of perovskite type oxides in them, classified attending to the oxidant used, ozone, H_2O_2 or peroxymonosulfate, alone or in combination with other systems. The photocatalytic oxidation, consisting in the activation of the perovskite by irradiation with ultraviolet or visible light is also revised.

Keywords: perovskites; advanced oxidation processes (AOPs); Fenton-like; peroxymonosulfate; heterogeneous photocatalysis

1. Introduction

Advanced oxidation processes (AOPs) are based on the generation of radical intermediates, mainly hydroxyl radicals (HO•), in amount enough to be able to attack and oxidize either partially or fully most of the recalcitrant chemicals present in the effluent water, such as pesticides, dyes, pharmaceuticals and so on [1]. The processes based on the free radicals occur at higher rates of degradation than those based on other chemical oxidation technologies and are not highly selective [2,3]. The high oxidation potential of hydroxyl radicals (2.80 v) make them capable of attacking organic compounds by abstracting a hydrogen atom or by adding to the double bonds, carrying out their mineralization by transformation into more oxidized intermediates, carbon dioxide, water and inorganic salts. These reactions of hydroxyl radicals with organic compounds can be written as follows:

$$HO\bullet + R\text{-}H \rightarrow H_2O + R\bullet \quad (1)$$

$$HO\bullet + C{=}C \rightarrow HO\text{-}C\text{-}C\bullet \quad (2)$$

$$HO\bullet + Ph\text{-}H \rightarrow Ph\text{-}H(OH)\bullet \quad (3)$$

AOPs can be classified in several categories, depending on the different reagent systems used for the generation of hydroxyl radicals. Attending to the reaction medium, these advanced oxidation processes can be classified either as homogeneous or heterogeneous [4]. The first ones can be subdivided in turn in those using energy (ultraviolet or visible radiation, ultrasound energy, electrical energy) and those not involving energy (ozone (O_3) in alkaline medium, O_3/H_2O_2 and H_2O_2/homogeneous catalyst, generally Fe^{2+}, known as Fenton process). The heterogeneous processes

can be classified in four main groups: (i) catalytic ozonation, which uses the combination of O_3 and a solid catalyst; (ii) photocatalytic ozonation, under the action of O_3/light (UV or visible)/solid catalyst; (iii) Fenton-like processes, which are produced by the action of H_2O_2/solid catalyst, containing mainly the Fe^{2+}/Fe^{3+} couple but also other transition metal ions with multiple oxidation states; when they are combined with the action of light they are called Photo-Fenton processes; and iv) photocatalytic oxidation, by combination of light (UV or visible) and a solid catalyst.

It must be remarked that the single ozonation or the use of only H_2O_2 belong to the class of chemical oxidation technologies, as they work on the direct attack of the oxidants, not being considered as AOPS, because they do no generate hydroxyl radicals by themselves [5]. Only when O_3 and H_2O_2 are combined between them or its individual action is supplemented by other dissipating energy components, such as UV/visible light or ultrasound or by activation with a catalyst, the formation of free radicals occurs and they can be considered AOPs.

In the last fifteen years some reviews in literature have devoted to show the state of art of AOPS for wastewater treatment [4–7] and in particular Fenton and photo-Fenton processes [8,9]. Most of these oxidation technologies are usually expensive and in addition, they are unable to completely degrade the organic compounds present in real wastewater and they cannot process the large volumes of waste generated. However, AOPs can degrade the residue up to a certain level of toxicity and then the intermediate can be furtherly degraded by the conventional methods. Furthermore, the combination of AOPs (as a pre-treatment or post-treatment stage) with a biological treatment contributes to reduce operating costs of the global process [10].

As mentioned above, the heterogeneous advanced oxidation processes generally use solid catalysts in combination with other systems (O_3, H_2O_2, light) to carry out the degradation of organics. The main advantage of heterogeneous catalysts with respect to the homogeneous ones is the facility of separation of the product and of the recovery of the catalyst. However, to be applied in the industry, heterogeneous catalysts must satisfy some specifications, such as high activity, thermal, mechanical, physical and chemical stability and resistance to the deactivation.

Perovskite-type oxides of the general formula ABO_3, where A is a rare earth metal and B a transition metal, have attracted the attention of many scientists because of their unique structural features. They have a well-defined structure, which allows the introduction of a wide variety of metal ions in both A and B positions [11,12]. Its structure is represented in Figure 1. The partial substitution of these cations by other foreign leads to changes in the oxidation states of metal ions and to the formation of oxygen vacancies. The thermal and hydrothermal stability of perovskites is quite high and as a result, they can be applied to gas or solid reactions carried out at high temperatures or liquid-phase reactions occurring at low temperatures [13,14]. The high mobility of network oxygen and the stabilization of unusual oxidation states confer them a diversity or properties, which allows their application as solid oxide fuel cells [15], magnetic and electrode materials [16], chemical sensors [17], adsorbents [18] and heterogeneous catalysts in industrial reactions [11,14,19]. One of the potential applications of perovskites is as catalysts in carbon-based electrodes, which has incited many scientists to study the mechanism of the catalytic decomposition of H_2O_2 by perovskites [20–22].

Catalysts used in oxidation technologies can be classified as follows: (i) metal catalysts, usually supported on a metal oxide surface (TiO_2, Al_2O_3, ZrO_2 and CeO_2) or on active carbon; (ii) metal oxide catalysts and (iii) organometallic catalysts. Different heterogeneous catalysts have been applied in some AOPs. As an example, the use of several heterogeneous systems containing iron species stabilized in a host matrix, such as oxides [23–26], clays [23,27–30], zeolites [29,31,32] or carbon materials [33–37] in the Fenton and the Fenton-like processes has been reported. In the last years perovskites have been applied as Fenton catalysts because of their versatile composition and high stability [19]. Furthermore, the existence of redox active sites in B cations and oxygen vacancies may facilitate the transformation of H_2O_2 into HO• [38–40].

There are some reviews in literature describing the employment of clays and mineral oxides, mainly of iron, in Fenton-like processes [23,25,26]. However, until our knowledge, there is no any

review reporting the use of perovskites in AOPs. In the present paper we describe the utilization of perovskites and like-perovskite oxides in this kind of processes, classified as a function of the oxidant reactant responsible for generating the free radicals, by alone or combined with other systems, giving place to the hybrid methods. Thus, in first place, in Section 2, we report the processes based on ozone, O_3, including catalytic ozonation (O_3/catalyst) and photocatalytic ozonation (O_3/catalyst/light). In the following section we revise the use of H_2O_2 as oxidant in three kinds or systems: (i) Fenton-like reactions (H_2O_2/catalyst); (ii) photo Fenton-like reactions (H_2O_2/catalyst/light); and (iii) catalytic wet peroxide oxidation, CWPO, (H_2O_2/catalyst/air). In the last fifteen years a new chemical oxidant, peroxymonosulfate (PMS), has aroused a great interest as alternative to others as H_2O_2 or O_3. For that reason, the fourth section is devoted to describing the use of PMS, activated by a catalyst (perovskite) or by the combination of both a catalyst and light irradiation. The photocatalytic oxidation, consisting in the activation of perovskite by irradiation with UV or visible light, is revised in Section 5. Finally, a short section devoted to the degradation under dark ambient conditions, show some examples in which perovskites catalyse the oxidation of organics in the absence of light and without additional chemical oxidant. Although these processes should not be considered strictly AOPS, because radicals are not formed, some authors consider them as novel advanced oxidation technologies for low cost treatment of wastewaters.

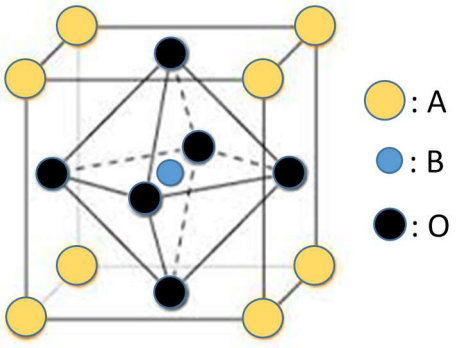

Figure 1. Unit cell of perovskite centred on A.

2. Processes Based on Ozone

Heterogeneous catalytic ozonation is getting an enormous attention in the treatment of drinking and waste water, because of its capacity to improve the mineralization and degradation of organic pollutants, its manufacturing simplicity and economic nature. There are many advantages to the use of ozone compared to other conventional technologies due to its high oxidizing power (2.07 V). Ozone can degrade organic pollutants by direct electrophilic attack with molecular ozone or by indirect attack with hydroxyl radicals HO•, which are generated through its decomposition process. Single ozonation has been widely used in water and wastewater because is an effective oxidation process. However, several disadvantages can limit its application such as slow and incomplete oxidation or mineralization (the intermediates are not totally oxidised to CO_2 and water) and the low solubility and stability of ozone in water. At first sight, heterogeneous catalytic ozonation does not present these drawbacks although much research is still needed. Catalytic ozonation utilizes solid catalysts in order to improve the decomposition of ozone and to enhance the production of hydroxyl radicals, HO•. In general, the heterogeneous catalysts decompose the ozone into caged or free radicals or simply they adsorb reactants facilitating their reaction. To date, several types of heterogeneous ozonation catalysts such as metal oxides, supported metal oxides and carbon materials have been tested with promising results. Perovskites-type metal oxides constitute undoubtedly an interesting alternative due to the high stability under aggressive conditions, high degree of stabilization of transition metals in their oxidation states and high oxygen mobility. However, the catalytic ozonation mechanism with perovskites is still a challenge for chemists and not many detailed studies are available. Most of the studies have been carried out by the same research group [41–44].

The first studies concerning catalytic ozonation with active perovskites appeared in 2006 [41]. The authors studied the ozonation decomposition of pyruvic acid, a refractory substance typically produced after oxidation of phenol-like compounds, in the presence of $LaTi_{0.15}Cu_{0.85}O_3$ perovskite. This perovskite was active and stable in the ozonation process being oxalic and acetic acids the only intermediates formed. Experimental results clearly indicated that typical operating parameters like ozone concentration, mass of catalyst or temperature, performed a key role on the pyruvic acid ozonation. The catalyst exhibited high stability and its catalytic activity improved after the first use. For instance, after 150 min of reaction the pyruvic acid had practically been eliminated, in contrast to the 67% of conversion achieved with fresh catalyst for the same period. Regarding kinetic considerations, authors proposed a Langmuir–Hinshelwood mechanism derived from bi-adsorption of pyruvic acid and ozone on different active sites and successive reaction of pyruvic acid with the O• radicals on the surface through reactions 1 and 2, before occurring the desorption of formed products (see Scheme 1).

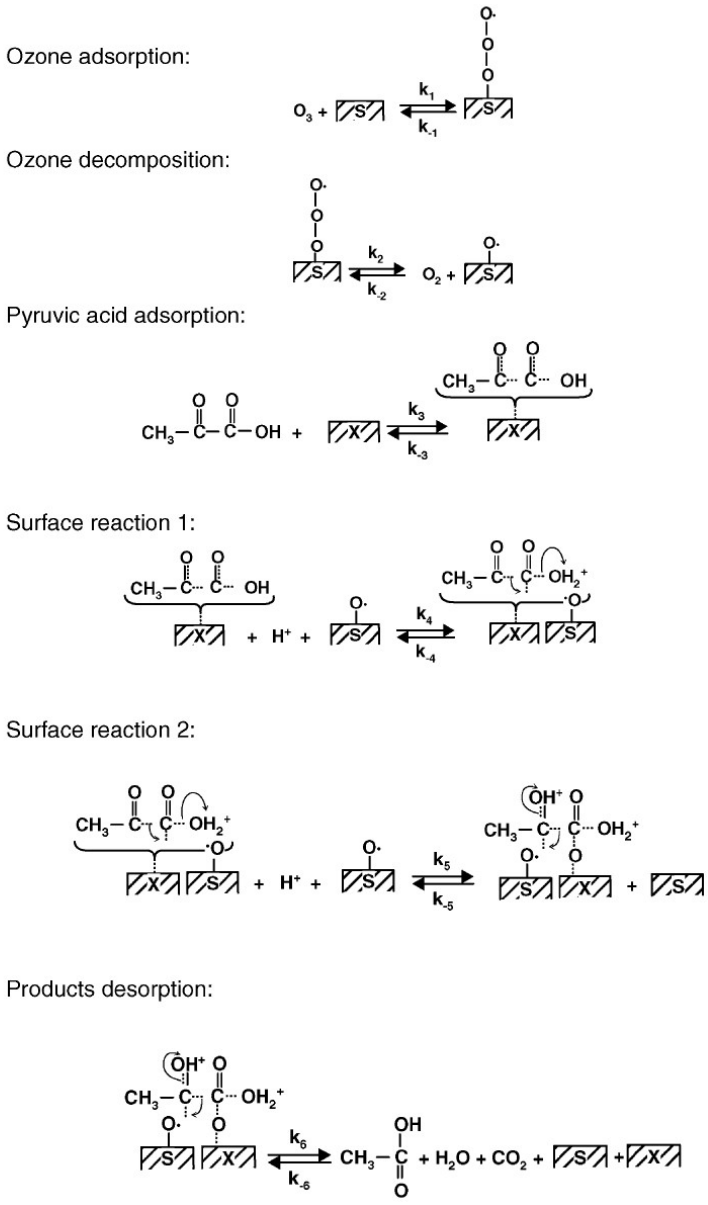

Scheme 1. Mechanism of catalytic ozonation of piruvic acid in the presence of $LaTi_{0.15}Cu_{0.85}O_3$. With permission from [41].

Carbajo et al. [42] extended the study of the removal of pyruvic acid from water through catalytic ozonation to other perovskites, $LaTi_{1-x}Cu_xO_3$ and $LaTi_{1-x}Co_xO_3$, which were compared with other catalysts, such as Ru-Al_2O_3, Ru-CeO_2, FeO(OH) and MCM-41, this last impregnated with copper or cobalt. The results showed that only perovskites and Ru-CeO_2 catalysts increased significantly the pyruvic acid depletion with respect to the produced in the absence of catalyst. Conversion values of 80% were reached after 2 h of catalytic ozonation. Due to the low adsorption capacity of the catalysts to adsorb the pyruvic molecules, authors concluded that the catalytic ozonation mechanism was governed by surface reactions involving adsorbed ozone and dissolved pyruvic acid.

Another pioneering work with $LaTi_{0.15}Cu_{0.85}O_3$, the same catalyst used in Reference [41], was carried out to eliminate gallic acid, a primary intermediate of benzoic acid oxidation [43]. The role of different operating variables was studied. Whereas the catalyst and ozone doses exerted a positive influence in the ozonation rate, the increment in the initial acid gallic concentration diminished the conversion. The activity of the catalyst in terms of acid elimination was kept for consecutive cycles. However, the catalyst displayed a partial deactivation in terms of total organic carbon (TOC) elimination after the second reuse. In any case, the TOC degree was still higher than the one achieved in the non-catalytic system.

Finally, Carbajo et al. [44] went a step further in analysing the activity of the same catalyst, $LaTi_{0.15}Cu_{0.85}O_3$, in the ozonation of four real phenolic wastewaters coming from agro-industrial field, a wine distillery industry, olive debittering and from olive oil production. The main goal was to study the activity and stability of the catalyst together with the influence of the different operating variables. The results suggested that if enough time was allowed the catalytic ozonation of the phenolic mixture achieved 100% of mineralization. Moreover, the increment of temperature promoted the mineralization level.

Some of the compounds that cannot be easily removed from drinking water or wastewater by classical treatments are pharmaceutical compounds. Catalytic ozonation allows high removal of organic carbon of these compounds being the most appropriate process. As a first approach Beltran et al. [45] tested two copper and cobalt perovskites, $LaTi_{0.15}Cu_{0.85}O_3$ and $LaTi_{0.15}Co_{0.85}O_3$, as catalysts to remove in the presence of ozone sulfamethoxazole, a synthetic antibiotic usually found in municipal wastewaters. Some experiments were also carried out in the presence of activated carbon, as promoter of the activation of ozone. The results showed that catalytic or promoted ozonation were not necessary to eliminate sulfamethoxazole from water, because it can be removed only by the action of ozone. However, from a practical point of view, the combined ozone processes are clearly recommended in order to remove the resulting total organic carbon (TOC). The catalytic ozonation of two pharmaceutical compounds, the drug diclofenac and the synthetic hormone 17-ethynylstradiol, was also conducted on the same perovskites by the same authors [46], obtaining similar results to those observed in their previous work. Both compounds can be eliminated by direct ozonation; however, when copper perovskite was used, the TOC removal reached the 90% after 2 h of reaction.

To date, the main advantage of catalytic ozonation is the ability to improve the mineralization degree achieved at the end of the process. In this sense, non-substituted perovskites type $LaBO_3$ (B=Fe, Ni, Co and Mn) and substituted perovskites type $LaB_xCu_{1-x}O_3$ (B=Fe and Al), have been proposed as effective catalysts in ozonation processes of oxalic acid and dye C.I. Reactive Blue 5 [47]. Most of perovskites tested showed better performances in the catalytic ozonation of oxalic acid than single ozonation. On the contrary, in the case of the removal of dye, conversion values reached through single ozonation were slightly higher than in catalysed systems. However, the results in terms of TOC removal were better in the presence of catalyst and $LaCoO_3$ allowed almost complete mineralization of dye after 3 h of reaction under the conditions tested. A key factor in the removal of contaminants seems to be the presence of lattice oxygen vacancies, which are able to activate adsorbed species.

In general, the catalytic activity seems to be enhanced by high surface area and easy access of reactants to the active sites. Then high surface area could be of interest to improve the activity of catalysts. Concerning to that, Afzal et al. [48] studied the behaviour of high surface area perovskites

for catalytic ozonation of 2-chlorophenol. A nanocasting technique (NC), using SBA-15 as a template, was employed for the synthesis of NC-$LaMnO_3$ and NC-$LaFeO_3$ catalysts, with high surface area. Authors compared these catalysts with the same perovskites synthesized by conventional citric acid (CA) assisted route, CA-$LaMnO_3$ and CA-$LaFeO_3$, as well as with Mn_3O_4 and Fe_2O_3. They found that NC-perovskites, containing easily accessible active sites, showed higher catalytic activity (80% of TOC removal) than their counterpart CA-perovskites (35% of TOC removal). Mn_3O_4 and Fe_2O_3 were the worst catalysts.

Bromide, Br−, is usually present as micro-emerging pollutant in some water matrixes to be degraded. The ozonation treatment leads to the formation of bromate, BrO_3^-, which is considered a potential carcinogen to humans by the World Health Organization, therefore being necessary its removal from the water. Zhang et al. [49] tested two perovskites, $LaCoO_3$ and $LaFeO_3$, as catalysts for the simultaneous removal of BrO_3^- and benzotriazole (BZT) in the presence of ozone. 71% of BrO_3^- was eliminated and BZT was completely degraded in only 15 min when $LaCoO_3$ was used. $LaFeO_3$ resulted in being inactive for BZT degradation; however, it reduced BrO_3^- to $HOBr/OBr^-$ efficiently. The surface hydroxyl groups present in both perovskites were key in the involved reactions.

When the catalytic ozonation does not lead to a high degree of mineralization, it is necessary to combine it with other oxidation systems. The integration of catalytic ozonation and photocatalysis seems to be the most appropriate solution [50]. Photocatalytic ozonation is an advanced ozonation route allowing high removal of organic carbon by combining the beneficial effects of ozonation with the generation of hydroxyl radicals via electron hole formation (free radical oxidation). Considering that perovskites have been successfully used in catalytic ozonation, some authors studied the O_3/UVradiation/perovskites system. Thus, Rivas et al. [51] carried out the advanced oxidation of pyruvic acid in presence of $LaTi_{0.15}Cu_{0.85}O_3$ with several oxidation systems: O_3, UV radiation, O_3/UV radiation, O_3/perovskite, UV radiation/perovskite, O_3/UV radiation/perovskite, H_2O_2/UV radiation, H_2O_2/UV radiation/perovskite, being O_3/UV radiation/perovskite the system investigated in more detail. The efficiency of the oxidation systems was examined in terms of the economic cost as a function of removal percentage of pyruvic acid and TOC. As expected, ozone was not able of eliminating pyruvic acid, displaying conversion values around 20% after 3 h of reaction. In contrast, application of UV radiation led to 40% of pyruvic acid elimination. Finally, for the combined O_3/UV radiation/perovskite system, the pyruvic acid removal reached 100%, while the mineralization degree obtained was 80%. Therefore, under the operating conditions investigated, the photocatalytic ozonation seems to be the best option.

3. Processes Based on Hydrogen Peroxide

3.1. Fenton-like Reactions (H_2O_2/catalyst)

The homogeneous Fenton system implies the reaction of Fe^{2+} with H_2O_2 to generate hydroxyl radicals (Equation (4)), with a high reactivity and high oxidant power, capable of oxidize organics according to Equations (1)–(3).

$$Fe^{2+} + H_2O_2 \rightarrow Fe^{3+} + HO\bullet + HO^- \quad (4)$$

The generated HO• radicals can re-combine with Fe^{2+}:

$$Fe^{2+} + HO\bullet \rightarrow Fe^{3+} + HO^- \quad (5)$$

The ferric ions formed may decompose the hydrogen peroxide into water and oxygen, following the Equations (6)–(10), in which ferrous ions and radicals are also generated. The reaction of H_2O_2 with Fe^{3+} is referred in literature as Fenton-like reaction [52].

$$Fe^{3+} + H_2O_2 \rightarrow Fe\text{-}OOH^{2+} + H^+ \quad (6)$$

$$\text{Fe-OOH}^{2+} \rightarrow \text{HO}_2\bullet + \text{Fe}^{2+} \quad (7)$$

$$\text{Fe}^{2+} + \text{HO}_2\bullet \rightarrow \text{Fe}^{3+} + \text{HO}_2{}^- \quad (8)$$

$$\text{Fe}^{3+} + \text{HO}_2\bullet \rightarrow \text{Fe}^{2+} + \text{O}_2 + \text{H}^+ \quad (9)$$

$$\text{HO}\bullet + \text{H}_2\text{O}_2 \rightarrow \text{H}_2\text{O} + \text{HO}_2\bullet \quad (10)$$

Other reactions involving radicals in the Fenton process are:

$$\text{H}_2\text{O}_2 + \text{HO}\bullet \rightarrow \text{HO}_2\bullet + \text{H}_2\text{O} \quad (11)$$

$$\text{HO}_2\bullet + \text{HO}_2\bullet \rightarrow \text{H}_2\text{O}_2 + \text{O}_2 \quad (12)$$

Notice that by reaction (11) H_2O_2 acts as sink for HO•, diminishing the oxidizing power of the Fenton reactants.

The homogeneous Fenton system, which implies the reaction of Fe^{2+}/Fe^{3+} in solution with H_2O_2, has several drawbacks. By one hand, the chemical reactivity of iron is strictly dependent on the pH and only at pH ≈ 3, all three Fenton-active species of Fe^{2+}, Fe^{3+} and $Fe(OH)^{2+}$ coexist together. On the other hand, the final effluent contains high metal concentrations, which have to be recovered by additional treatment. In the heterogeneous systems Fe^{2+} and Fe^{3+} are part of a solid, which results in different advantages, especially related to recovery of the catalyst and the low leaching of ions.

The Fenton-like reactions involved in a heterogeneous system are the following:

$$\text{S-Fe}^{2+} + \text{H}_2\text{O}_2 \rightarrow \text{S-Fe}^{3+} + \text{HO}\bullet + \text{HO}^- \quad (13)$$

$$\text{S-Fe}^{3+} + \text{H}_2\text{O}_2 \rightarrow \text{S-Fe}^{2+} + \text{HO}_2\bullet + \text{H}^+ \quad (14)$$

$$\text{S-Fe}^{2+} + \text{HO}\bullet \rightarrow \text{S-Fe}^{3+} + \text{HO}^- \quad (15)$$

$$\text{S-Fe}^{3+} + \text{HO}_2\bullet \rightarrow \text{S-Fe}^{2+} + \text{O}_2 + \text{H}^+ \quad (16)$$

$$\text{Organic} + \text{HO}\bullet \rightarrow \text{R}\bullet + \text{H}_2\text{O} \rightarrow \ldots \rightarrow \text{CO}_2 + \text{H}_2\text{O} \quad (17)$$

where S represents the surface of the catalyst. The reaction (14) is rate-limiting since its rate constant is ca. four orders of magnitude lower than that of reaction (13).

Although the classical Fenton system is based on the use of Fe^{2+}/H_2O_2, other elements with multiple redox sates (like chromium, cerium, copper, cobalt, manganese and ruthenium) can directly decompose H_2O_2 into HO• through conventional Fenton-like pathways [53]. Therefore, perovskites containing these elements, mainly in B position, can be used in this kind of reaction.

Rhodamine B (RhB) is one of the most studied organic pollutants in water in the Fenton-like reactions [54–58]. The first study reporting the use of perovskites as catalysts for the removal of RhB in Fenton-like reactions was carried out by Luo et al. [54]. In this work, $BiFeO_3$ magnetic nanoparticles (BFO MNPS) prepared by sol-gel method were tested in the degradation of RhB in the presence of H_2O_2 at 25 °C and pH = 5. According to the isoelectric point of BFO MNPs (I.P. = 6.7), under these conditions, the anionic form of the dye (pKa = 3.7) interacts easily via electrostatic forces with the positively charged catalyst particles. By selecting initial H_2O_2 and catalyst concentrations as 10 mM and 0.5 g/L, respectively, 95.2% of RhB was degraded in 90 min and a TOC removal of 90% was achieved within 2 h, in contrast to the removal of only 10% of RhB in the presence of Fe_3O_4 nanoparticles. By Montecarlo (MC) simulations authors concluded that after the adsorption of H_2O_2 molecules on the surface hollow sites of BFO MNPs facets, they are activated to generate HO• radicals, which then decompose RhB into other smaller organic compounds and CO_2. BFO MNPs showed excellent chemical stability during reaction (as checked by XPS), being reusable for at least five cycles, without a significant loss of activity. BFO MNPs were also tested in the degradation of methylene blue and phenol, leading to 79.5% and 82.1% of removal, respectively.

Zhang et al. [55] synthesized a series of Cu-doped $LaTiO_3$ perovskite ($LaTi_{1-x}Cu_xO_3$, x = 0.0–1.0) by a sol-gel method, which resulted be very efficient for the degradation of RhB with H_2O_2 in a pH range of 4–9. In contrast to the absence of activity of sample containing only titanium, the coexistence of Ti^{3+}/Ti^{4+} and Cu^{+}/Cu^{2+} in the perovskite structure of partially substituted samples allowed the degradation of 8 mg/L of RhB through redox cycles involving the transformation of H_2O_2 into HO• and $HO_2•/O_2•^-$. For a H_2O_2 concentration of 10 mM, about 84% of RhB was decolorized within 2 h in the presence of 1.4 g/L of $LaTi_{0.4}Cu_{0.6}O_3$. Notice that the amount of RhB degraded was slightly lower than the observed by Luo et al. [54]; although the catalyst amount used in Reference [55] was almost three times higher, the initial concentration of RhB was approximately the double. The reduction of H_2O_2 to O_2, which is carried out by oxygen vacancy [22], was not observed in this reaction.

The surface area of perovskites is low and as a consequence, the interaction between the contaminants and the active sites is limited. In order to improve the catalytic efficiency of perovskite-like oxides by increasing their surface area, some strategies have been developed, such as their supporting on mesoporous silica supports [56–58] or in honeycombs [59] and the formation of nanocomposites [60,61].

In this sense, La-FeO_3/SBA-15 [56] was more efficient than non-supported $LaFeO_3$ for catalysing RhB oxidation in the presence of H_2O_2 under ambient conditions due to a synergic effect between the large capacity of mesoporous SBA-15 for RhB adsorption and the high number of active sites exposed in $LaFeO_3$ nanoparticles for reacting with H_2O_2. The best catalyst was the sample containing many oxygen vacancies (as deduced from XPS results), which are a key factor influencing the performance of these catalysts in oxidation reactions. The catalyst was efficient in a wide pH range (2–10). Under the optimum conditions, a degradation of RhB of 87% was achieved after 3 h. No leaching of Fe^{3+} was observed in the solution after reaction, the contribution of homogeneous Fenton reaction being discarded. The stability of La-FeO_3/SBA-15 was also confirmed by carrying out four cycles of reutilization, which showed no deactivation of the sample. The catalyst was also applied for the degradation of other organic dyes, achieving a decomposition of 66% for methylene blue and 42% for brilliant red X-3B and direct scarlet 4BS.

The good synergy between the support and the $LaFeO_3$ perovskite was explored by the same authors [58], who tested different supports based on mesoporous silica, such as SBA-15, SBA-16 and MCF and on nanosized silica powders (NSP). Different factors influence on the catalytic behaviour for degradation of RhB. By one hand, the RhB adsorption on the support is a crucial step of the reaction and as a result, the combination of $LaFeO_3$ with a non-porous support showing a low capacity of adsorption decomposed the RhB in a little extent. On the other hand, a network of pores with short length is necessary to allow the transportation of RhB to the active sites of $LaFeO_3$. In this sense, the shorter the pore length, the faster the RhB molecules reached the catalytic centres and were oxidized (see the transport process in Figure 2). Authors concluded that $LaFeO_3$ supported on MCF containing randomly distributed pores with short length was the best catalyst for oxidative degradation of RhB in aqueous solution, achieving a removal of the contaminant of 97% in 2 h.

SBA-15 was also used by the same authors as support of a perovskite-type oxide La_2CuO_4 containing a few amounts of CuO [57]. The solid was tested in the degradation of RhB and organic dyes, including reactive brilliant red X-3B, direct scarlet 4BS and methylene blue under ambient conditions. The catalyst was active in a wide pH range (2–10) and depletion of RhB between 85% and 95% was produced after 3 h, depending on the amount of catalyst. The mineralization of RhB into CO_2 was completed and the catalyst could be recycled. Although the activity decreased in ca. 14% in the fifth cycle, it could be recovered after a treatment of the used catalyst in air at 500 °C for 2 h.

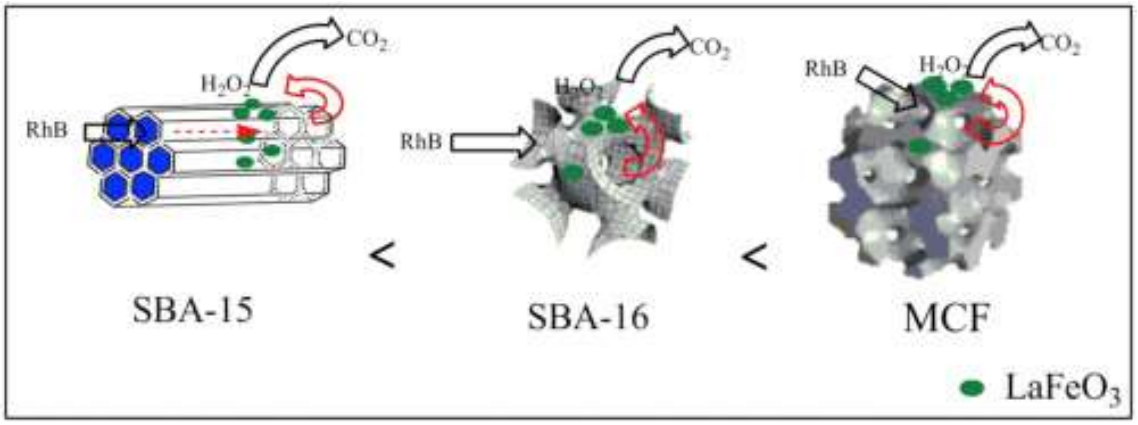

Figure 2. A proposed scheme of transporting RhB from the solution to the pore and then to the surface-active site over $LaFeO_3$ catalysts supported on porous SBA-15, SBA-16 and MCF. With permission from [58].

Another approach for modifying the surface properties and reactivity of perovskites is the formation of nanocomposites [60,61]. In this regard, a novel 3D perovskite-based composite $BiFeO_3$/carbon aerogel (BFO/CA) prepared by sol-gel method led to a 95% of degradation of ketoprofen in 150 min and a TOC removal of 60% after 5 h [60]. These activities values were significantly higher than those obtained for bulk BFO and nano BFO, due to the higher reducibility of Fe^{3+} and Co^{3+} species in the composite, as deduced from TPR studies and to the dispersion of active sites not only on the surface of CA support but along the 3D structure of CA. Furthermore, the catalyst was active in a wide pH range of 3–7 and the leaching of iron was low.

A $La_{1+x}FeO_3$ ($L_{1+x}FO$, $0 \leq x \leq 0.2$) nanocomposite formed between $LaFeO_3$ and an inert La_2O_3, resulted to be twice more active for degradation of methyl orange that the pristine $LaFeO_3$ [61]. The modification of surface properties, such as surface Fe^{2+} concentration, surface defects, H_2O_2 adsorption capacity and charge-transfer rate led to an enhanced Fenton-like activity in the composite. The most notorious aspect of this work was that the major reactive species were not hydroxyl radicals but singled oxygen ($^1O_2$), as deduced from in situ electron paramagnetic resonance analysis and radical scavenging experiments. Authors proposed the corresponding mechanism of $^1O_2$-based composite/H_2O_2 system. 100% of contaminant was degraded in 90 min at pH = 3 and a total organic carbon (TOC) removal of 96% was achieved after 4 h.

Other contaminants degraded by $LaFeO_3$ perovskite, in this case auto supported, were different pharmaceutical and herbicides [62]. Among them, sulfamethoxazole (SMX) was completely removed in $LaFeO_3$–H_2O_2 system after 2 h at neutral pH. By formation of a surface complex between $LaFeO_3$ and H_2O_2, the O-O bond in H_2O_2 is weakened and chemical environment of iron changes, the Fe^{3+}/Fe^{2+} redox potential decreasing significantly, which accelerates the cycle of Fe^{3+}/Fe^{2+} and produces more HO• and $O_2•^-$ / HO_2• radicals, enhancing the Fenton-like removal of organic compounds. The TOC removal was 22% in 2 h and SMX was transformed into simpler aliphatic acids, mostly biodegradable.

Due to its abundance in most of wastewater effluents and its toxicity, phenol is a usual organic compound model in developing methods for water remediation, including AOPs. The removal of phenol and phenolic compounds has been tested in Fenton-like reactions on different perovskites, mainly containing iron or copper in B position [63–65]. $LaFeO_3$ and $BiFeO_3$ were tested by Rusevova et al. [63] in the degradation of phenol. The influence of reaction temperature, catalyst and H_2O_2 concentrations and pH, on the catalytic behaviour was studied. The rate constant for phenol degradation, which increased with temperature, was 3-fold higher when initial reaction pH diminished from 7 to 5. Conversion values of phenol of 90–95% were achieved after 6 h and leaching of metals was negligible. The most new-fangled aspect of the study was that in order to settle the nature of the active oxidizing species authors used compound specific stable isotopic analysis (CSIA) as alternative to other conventional techniques. Based on their results, authors concluded that the major species involved in

phenol degradation were hydroxyl radicals. They extended the application of both $LaFeO_3$ and $BiFeO_3$ to the removal of methyl terc-butyl ether (MTBE), for which a depletion of 80% was obtained after 6 h.

Different perovskite-like oxides $LaBO_3$ (B = Cu, Fe, Mn, Co, Ni) synthesized using the Peccini method were tested in Fenton-like degradation of phenol but only $LaCuO_3$ and $LaFeO_3$ were active [64]. Authors studied the recyclability of the catalysts during 3 cycles for $LaCuO_3$ and 40 cycles for $LaFeO_3$.The induction period observed in the first cycle for $LaFeO_3$ was significantly shortened for the second and successive cycles. In this sense, a degradation of phenol of 75% was produced in 5 h in the second cycle, in contrast to the 22% observed in the first one. The reasons for this improvement in the activity were an increase in the surface concentration of oxygen containing species (water and carbonate) involved in the transformation and the formation of dispersed particles of iron oxides on the surface. The TOC conversion of 21–22% after 10 h did not change for the different cycles.

Hammouda et al. [65] prepared ceria perovskite composites CeO_2-$LaCuO_3$ and CeO_2-$LaFeO_3$, which were more active for the degradation of bisphenol than non-doped perovskites, especially at short reaction times. Furthermore, CeO_2 improved the stability of perovskites towards leaching of metals. Authors attributed the enhancement in the activity to the fact that, as observed by XPS, more Ce^{3+} ions were formed in the ceria-perovskite catalysts, due to an electron transfer from the transition metal of perovskites to the CeO_2. As a result, more oxygen radicals were formed by interaction of H_2O_2 with Ce^{3+}, favouring the Fenton-like degradation of the contaminant. By following the evolution of the intermediates formed, authors proposed a mechanism of reaction and a degradation pathway.

In order to improve the catalytic ability of $BiFeO_3$ nanoparticles to degrade recalcitrant pollutants, some authors have proposed an in-situ surface modification by using chelating agents [66,67]. In this regard, the bisphenol A (BPA) degradation in a wide pH range (4–9) was accelerated when the nano-$BiFeO_3$ were modified by adding different ligands to the Fenton solution, such as tartaric acid, formic acid, glycine, nitrilotriacetic acid and ethylenediaminetetraacetic acid (EDTA) [66]. EDTA was the most efficient chelating agent, mainly because of a higher HO• formation from the H_2O_2 decomposition. Under the optimum conditions 91.2% of BPA was removed within 2 h, in contrast to the 20% of BPA degraded with unmodified BFO. Although the use of chelating agents increased the contribution of Fenton homogeneous reaction by formation of soluble iron complexes, the trend observed in the BPA degradation for reactions carried out with different ligands did not follow the order of leached ions, indicating the irrelevant contribution of homogenous reaction to BPA degradation. As EDTA was the most efficient chelating agent, it was also used by same authors [67] as ligand for $BiFeO_3$ in the degradation of triclosan (5-chloro-2-(2,4-dichlorophenoxy)phenol), a broad-spectrum antibacterial agent widely used in personal and health care products. When pristine BFO were used, triclosan was mainly transformed into 2,4-dichlorophenol, a carcinogenic compound. The addition of EDTA modified significantly the dechlorination ratio of triclosan, which increased from 26.4% for H_2O_2-BFO sample up to 97.5% in the chelated system. Triclosan was degraded almost completely in 3 h under the optimal conditions.

Another strategy to improve catalytic activity of perovskites in AOPs is the hetero-doping in order to produce more active sites of the low-valence B-site transition metals (i.e., Fe^{2+}, Cu^{+} and Ti^{3+}) or to introduce oxygen vacancies, which can facilitate the transformation of H_2O_2 into HO• [39,40]. In this sense, some perovskites containing partially substituted manganese in B position, have been tested in Fenton-like reactions for the degradation of methylene blue (MB) [68], different dyes [69] and paracetamol [70].

Maghalaes et al. [68] tested $LaMn_{1-x}Fe_xO_3$ and $LaMn_{0.1-x}Fe_{0.9}Mo_xO_3$ perovskites in the decomposition of H_2O_2 to O_2 and in the oxidation of MB. The presence of manganese in the perovskites seemed to play an important role on the H_2O_2 decomposition rate, which decreased with the amount of Mn substituted by Fe and/or Mo. However, $LaMnO_3$ was not active for the MB discoloration, which suggested that it was able to transform the H_2O_2 into O_2 but it was unable to form the HO• radicals, necessary to degrade the dye molecules. On the contrary, samples substituted by Mo degraded MB up to 20% in 1 h.

Jahuar et al. [69] synthesized a series of manganese-substituted lanthanum ferrites having compositions $LaMn_xFe_{1-x}O_3$ (x = 0.1–0.5) by a sol–gel auto-combustion method, which were used as catalysts in the removal of anionic dyes (Remazol Turquoise Blue, Remazol Brilliant Yellow) and cationic dyes (MB, Safranine-O) by the action of H_2O_2, in the absence and presence of visible-light. The initial pH of solution was fixed in all cases to the value of 2. Unsubstituted $LaFeO_3$ produced a low dye degradation for long time periods, exhibiting a poor catalytic activity under dark conditions. However, the partial substitution of iron by manganese led to catalysts able to degrade over 90% of dye in time periods of 150–300 min, due to the Fenton-like activity of manganese ions, capable of existing in various oxidation states. In the presence of light, an enhancement in the catalytic activity was produced and degradation times were reduced to 25–70 min.

The contribution of manganese ions to Fenton-like reaction was, on the contrary, discarded by Carrasco-Díaz et al. [70] in the decomposition of paracetamol by H_2O_2 under mild reaction conditions (25 °C and pH $\approx$ 6) in the presence of $LaCu_xM_{1-x}O_3$ ($0.0 \leq x \leq 0.8$, M = Mn, Ti) perovskite-like oxides prepared by amorphous citrate decomposition. Degradation values of paracetamol between 80% and 97% were achieved after 5 h. XPS studies of the catalysts allowed authors to conclude that Cu^{2+}/Cu^{+} were the catalytically active species, the catalysts containing a higher amount of copper at the surface, mainly as Cu^{2+}, being the most active. The titanium and manganese species seemed not to be responsible of the enhanced activity observed in some of the substituted samples with respect to that of $LaCuO_3$. The catalysts were recyclable for at least three cycles and a negligible leaching of metals was produced. TOC values of 47–54% were achieved.

Finally, some mathematical analysis of the heterogeneous oxidations of contaminants by perovskites have been carried out. More concretely, mathematical modelling of photo-Fenton-like oxidation of acetic acid by $LaFeO_3$ has been reported [71,72]. From the experimental results authors concluded that the main reactions occurring in the system were the complete mineralization of acetic acid by H_2O_2 due to the presence of the catalyst and the decomposition of H_2O_2 into water and O_2 in the homogeneous phase. Therefore, this kind of reaction should not be considered as an AOP, because no hydroxyl radicals were formed.

Table 1 summarizes the conversion values and reaction conditions for the use of perovskites in the degradation of different organics by Fenton-like reactions and photo Fenton-like reactions, these last being revised in the following section.

Table 1. Oxides type perovskite used in Fenton-like and photo Fenton-like reactions of organic pollutants in aqueous solution.

			Concentration			Treatment Efficiency	
Reference	**Catalyst**	**Target Pollutant**	**Catalyst**	**Pollutant**	**H_2O_2**	**Degradation of Pollutant**	**TOC Removal**
[54]	$BiFeO_3$	RhB, phenol, MB	0.5 g/L	4.79 g/L	10 mM	95.2% (RhB) in 90 min	90% in 2 h
[55]	$LaTi_{1-x}Cu_xO_3$ (x = 0.0–1)	RhB	1.4 g/L	8 g/L	10 mM	84% in 2 h	-
[56]	$LaFeO_3$/SBA-15	RhB, MB, brilliant red X-3B, direct scarlet 4BS	2 g/L	9.1 mg/L	0.34 mM	87% in 3 h (RhB) 66% MB 42% for the others	-
[57]	La-Cu-O/SBA-15	RhB and other dyes	Not indicated, [RhB]/[catalyst]= 0.0045, 0.077	-	-	85-95% in 3 h	100% in 3 h
[58]	$LaFeO_3$/SBA-15, SBA-16, MCF and non-porous silica	RhB	2 g/L	9.6 mg/L	0.34 mM	97% in 2 h for $LaFeO_3$/MCF	-
[60]	$BiFeO_3$/carbon aerogel (BFO/CA)	ketoprofen	0.3 g/L	40 mg/L	12 mM	95% in 150 min	60% in 5 h
[61]	$La_{1+x}FeO_3$ ($L_{1+x}FO$, $0 \leq x \leq 0.2$) nanocomposite	Methyl orange	0.5 g/L	5 mg/L	0.198 M	100% in 90 min (pH 3)	96% in 4 h
[62]	$LaFeO_3$	Different herbicides and pharmaceutical	1.4 g/L	3 mg/L	23 mM	100% of SMX in 2 h (pH 6.5)	22% in 2 h
[63]	$LaFeO_3$, $BiFeO_3$	phenol, MTBE	0.01–1 g/L	25 mg/L phenol 50 mg/L MTBE	3 g/L = 88 mM	90–95% phenol in 6 h 80% MTBE in 6 h	-
[64]	$LaBO_3$ (B= Cu, Fe, Mn, Co, Ni)	phenol	5 g/L	0.01 M	0.7 M	85% in 10 h	21% in 10 h
[65]	Ceria-$LaCuO_3$, ceria-$LaFeO_3$	Bis-phenol	0.2 g/L	20 mg/L	10 mM	98% in 45 min (ceria-$LaCuO_3$) 92% in 42 min (ceria-$LaFeO_3$)	-
[66]	$BiFeO_3$ modified by chelating agents	BPA	0.5 g/L	0.1 mM	10 mM	91.2% in 2 h	-
[67]	$BiFeO_3$ (BFO); BFO modified by EDTA	Triclosan	0.5 g/L	34.5 mM	10 mM	82.7% in 3 h (BFO) 100% in 30 min (BFO-EDTA)	-
[68]	$LaMn_{1-x}Fe_xO_3$, $LaMn_{0.1-x}$ $Fe_{0.9}Mo_xO_3$	MB	30 mg (volume not indicated)	0.1 g/L	2.9 mM	20% in 1 h ($LaMn_{0.01}Fe_{0.9}Mo_{0.09}O_3$)	-
[69]	$LaMn_xFe_{1-x}O_3$ (x = 0.1–0.5), absence and presence of visible light	Anionic and cationic dyes	0.2 g/L	15 mg/L cationic dyes 60 mg/L anionic dyes	17 mM	Anionic dyes: 66–98% in 4 h (no light); 90–95.8 in 70 min (light) Cationic dyes: 90–99.4% in 5 h (no light); 98–99.7% in 30 min (light)	-

Table 1. *Cont.*

			Concentration			Treatment Efficiency	
Reference	**Catalyst**	**Target Pollutant**	**Catalyst**	**Pollutant**	**H_2O_2**	**Degradation of Pollutant**	**TOC Removal**
[70]	$LaCu_xM_{1-x}O_3$ ($0.0 \leq x \leq 0.8$, M= Mn, Ti)	paracetamol	0.2 g/L	50 mg/L	13.8 mM	80–97% in 5 h	47–54% in 5 h
[73]	$LaMnO_3$ +UV light	phenol	0.6 g/L	0.1 g/L	14.8 mM	99.92% in 4 h	-
[74]	Catalyst ($Bi_{0.97}Ba_{0.03}FeO_3$, $BiFe_{0.9}Cu_{0.1}O_3$, $Bi_{0.97}Ba_{0.03}$ $Fe_{0.9}Cu_{0.1}O_3$) + visible light	2-chlorophenol	0.4 g/L	50 mg/L	10 mM	100% in 70 min ($BiFe_{0.9}Cu_{0.1}O_3$, $Bi_{0.97}Ba_{0.03}$ $Fe_{0.9}Cu_{0.1}O_3$) 63% in 70 min ($Bi_{0.97}Ba_{0.03}FeO_3$)	68% in 1 h ($BiFe_{0.9}Cu_{0.1}O_3$) 73% in 1 h ($Bi_{0.97}Ba_{0.03}$ $Fe_{0.9}Cu_{0.1}O_3$)
[75]	$EuFeO_3$ (EFO) + visible light	RhB	1 g/L	5 mg/L	0.2 mM	37% EFO+vis. light 50% EFO+ H_2O_2 71% EFO+ H_2O_2+ vis. light	-
[76]	$LaFe_{1-x}Cu_xO_3$ + visible light	Methyl orange	0.8 g/L	10 mg/L	8.8 mM	92.9% in 1 h	-
[59]	$LaFeO_3$ + UV light $Pt/LaFeO_3$ + UV light	tartrazine	81.25 g/L	40, 60, 80 mg/L	0.0019–0.0076 mol/h	43% in 3 h ($LaFeO_3$) 63% in 3 h ($Pt/LaFeO_3$) (40 mg/L and 0.0038 mol/h) 100% in 30 min (catalyst + UV light)	45% in 3 h ($LaFeO_3$); 65% in 3 h ($Pt/LaFeO_3$) (40 mg/L and 0.0038 mol/h) 100% in 40 min (catalyst + UV light)
[77]	$LaMeO_3$ (Me= Mn, Co, Fe, Ni, Cu)(cordierite, and $Pt/LaMnO_3$/cordierite	acetic acid	9.4–40 g/L	1.26 g/L	83 mM	-	54% in 5 h ($Pt/LaMnO_3$) 60% in 5 h ($LaFeO_3$)
[78]	$LaFeO_3$/corundum with different loads of $LaFeO_3$	acetic acid, ethanol, acetaldehyde, oxalic acid	93.75 g/L	0.5 g/L	83 mM	-	97% (acetic acid); 53% (ethanol); 62% (acetaldehyde) and 95% (oxalic acid) in 5 h
[79]	$LaFeO_3$/corundum	MTBE	9.4–4 g/L	0.5 g/L	0–42 mM	-	100% in 2 h
[80]	$LaFeO_3$, $BiFeO_3$, $LaTi_{0.15}$ $Fe_{0.85}$ O_3 and $BiTi_{0.15}$ $Fe_{0.85}$ O_3	methylparaben	0.1 g/L	5 mg/L	0.5 mM	82.8% in 90 min	-
[81]	graphene-$BiFeO_3$+ + EDTA + visible light	TTBBA	0.5 g/L	0.011 g/L	20 mM	80% in 15 min	62.8% in 3 h

RhB: Rhodamine B; MB: Methylene Blue; MTBE: methyl tert-butyl ether; BPA: bis-phenol A; TTBBA: tetrabromobisphenol A.

3.2. Photo Fenton-Like Reactions (H_2O_2/Catalyst/Light)

In the photocatalytic oxidation processes, the electron–hole pairs in the catalyst are produced via the irradiation of the UV light and the oxidative radicals are formed between the catalyst and water interface [82]. The formation rate of HO• radicals in photo-Fenton processes is higher than in Fenton processes. While the Fenton reaction is governed principally by Equation (4) leading to the formation of HO• radicals, in the Photo-Fenton process occurs, in addition, the photolysis of H_2O_2:

$$H_2O_2 + h\nu \rightarrow 2\ HO\bullet \quad (18)$$

and the photo reduction of Fe^{3+}:

$$Fe^{3+} + H_2O + h\nu \rightarrow HO\bullet + Fe^{2+} + H^+ \quad (19)$$

Different perovskite oxides, non-supported [69,73–76], supported on monoliths [59,77–80] or in form of composites [81], have been used as catalysts for the degradation of several organics in the presence of H_2O_2 under light irradiation conditions.

A $LaMnO_3$ perovskite prepared by co-precipitation method resulted to be an excellent photo-Fenton catalyst of oxidation of phenol [73]. The phenol conversion (99.92% in 4 h) obtained when $LaMnO_3$ was activated by UV radiation in the presence of stoichiometric amount of H_2O_2 necessary to degrade phenol, was even higher than the achieved when using TiO_2 as catalyst (98% in 4 h). Furthermore, $LaMnO_3$ could be regenerated by calcination after reaction, yielding to similar catalytic performance to that of the first cycle.

In Reference [75] a series of iron perovskites containing europium in B position, $EuFeO_3$ (EFO), calcined at different temperatures, was used for the photodegradation of RhB by combination of visible light and H_2O_2. By the action of visible light, electron-hole pairs were formed in EFO nanoparticles and electrons were easily trapped by H_2O_2, leading to the formation of HO• radicals. In addition, a complex between Fe^{3+} at the surface ($\equiv Fe^{3+}$) and H_2O_2 was formed and $\equiv Fe^{3+}$ was transformed into $\equiv Fe^{2+}$, generating HO• and HO_2•, which decomposed RhB. Authors studied the effect of the calcination temperature of the catalysts on the band gap, microstructure and photocatalytic activity. The perovskite calcined at 750 °C showed the best catalytic behaviour, due to the combination of good crystallinity and appropriate BET surface area and band gap. The photodegradation of 37% of RhB after 3 h increased up to the 71% when H_2O_2 was added, which proves the Fenton-like activity of EFO nanoparticles.

One strategy to improve photocatalytic activity of ABO_3 perovskites is the substitution of the element in A or B position, which leads to the introduction of defects into the narrow band gap and to the formation of oxygen vacancies, which inhibit the recombination between the photogenerated electrons and the holes. In this regard, 2-chlorophenol (2-CP), was degraded in the presence of three metal doped $BiFeO_3$ (BFO) nanoparticles, H_2O_2 and visible light [74]. $BiFeO_3$ perovskite was substituted either in A position ($Bi_{0.97}Ba_{0.03}FeO_3$) or B position ($BiFe_{0.9}Cu_{0.1}O_3$) and in both ($Bi_{0.97}Ba_{0.03}Fe_{0.9}Cu_{0.1}O_3$). After only 70 min of visible light irradiation, Cu-doped BFO and Ba-Cu co-doped BFO almost completely removed 2-CP. The mineralization degree reached was of 68% and 73%, respectively. Authors concluded that in addition to the participation of Fe^{2+}/Cu^+ couple active for the formation of HO•, the oxygen vacancies on the surface can also participate by activating H_2O_2 molecules to form a lattice oxygen, which is furtherly desorbed as O_2.

More recently Phan et al. [76] studied the efficiency of $LaFeO_3$ (LFO) perovskites, doped with Cu in B position ($LaFe_{1-x}Cu_xO_3$), in the photo-Fenton decolorization of methyl orange (MO). Interestingly, the substitution of Cu into Fe-site in LFO modified the light absorption property of perovskite, as noted in the UV–vis absorption spectra and the corresponding band gap energy of LFO and $LaFe_{1-x}Cu_xO_3$ shown in Figure 3a,b, respectively. Notice that all the samples had suitable band gap energy for organic pollutant degradation under visible light irradiation. When Fe was substituted by 15 mol% of Cu

(LFO-15Cu), the MO degradation rate was improved in ca. 60% and 92.9% of MO was removed in only 1 h at an initial solution pH of 6. Under the optimum conditions, the photocatalytic performance of LFO-15Cu was also evaluated for two cationic dyes, rhodamine B (RhB) and methylene Blue (MB), obtaining even better results: 99.4% of degradation for RhB and 98.8% for MB in 60 min.

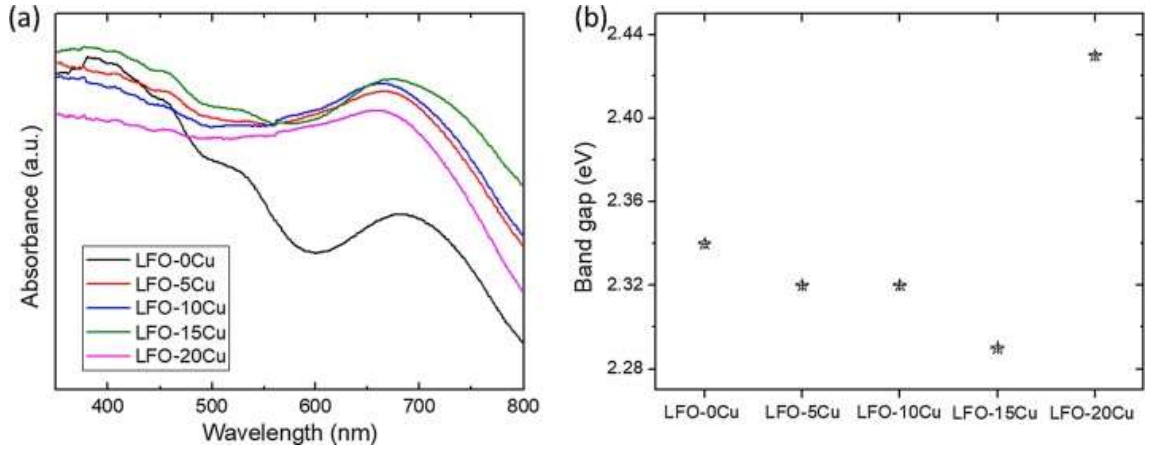

Figure 3. (**a**) UV–vis absorption spectra and (**b**) corresponding band gaps of LFO and $LaFe_{1-x}Cu_xO_3$. With permission from [76].

$LaFeO_3$ or $Pt/LaFeO_3$ perovskites supported on honeycomb monoliths have been tested in the degradation of tartrazine, a not-biodegradable dye used in food industries [59] by continuous flow of H_2O_2 in the presence of UV light at different pH values. The natural pH of solution (near 6) was the best operating condition, under which 100% of tartrazine was discoloured after 30 min of irradiation and mineralization was complete after 40 min. On the contrary, the discoloration was 50% under acidic condition (pH 3) and 55% under basic condition (pH 9), after 30 min of irradiation. In the first case, the excess of H^+ could react with HO• and produce water subtracting hydroxyl radicals necessary for the decomposition of tartrazine [83]. In the second one, H_2O_2 was accumulated in liquid medium because under alkaline conditions H_2O_2 has a very high stability [84] and as a consequence, the production of hydroxyls radicals was limited.

Supported $LaMeO_3$ (Me= Mn, Co, Fe, Ni, Cu) perovskites were prepared by impregnation of thin wall of monolithic honeycomb cordierite support with different active phase loadings and tested in the photo-Fenton oxidation of acetic acid [77]. In the case of $LaMnO_3$ sample, the honeycomb was also impregnated with 0.1% of Pt. Photo-Fenton activity was closely related to the amount of active phase supported on monolithic carrier and $LaFeO_3$ and $Pt/LaMnO_3$ perovskites were the best catalysts in terms of reaction rate. The addition of Pt enhanced the initial rate of acetic acid degradation, achieving the highest TOC removal, 18% in 1 h; however it did not enhance the catalytic performance after 5 h.

Different loads of $LaFeO_3$ perovskites supported over corundum monoliths were studied by the same authors in the photo-Fenton degradation of several organics [78] under UV irradiation. 97% of TOC removal was attained in the degradation of acetic acid after 4 h with the catalyst containing 10.64 wt% of $LaFeO_3$ and values of 53, 62 and 95% were achieved when ethanol, acetaldehyde and oxalic acid, respectively, were used as model pollutant.

The excellent catalytic behaviour of this catalyst was extended to other contaminants, as methyl terc-butyl ether (MTBE) [79]. About 100% of TOC removal and complete mineralization of MTBE into CO_2 and water was achieved if H_2O_2 was continuously dosed during irradiation time of 2 h at solution pH of 6.7. Although the TOC removal obtained by the combination of H_2O_2 and UV light in the absence of catalyst was quite high (about 97%), a very significant formation of CO was observed, indicating the importance of $LaFeO_3$ for the improvement in the mineralization of MTBE.

The degradation of methylparaben was studied in the presence of four ABO_3 perovskite catalysts (A: La, Bi and B: Fe, Ti-Fe) supported on a monolithic structure [80]. $BiFeO_3$ was the best catalyst and

under the optimum conditions 82.8% of pollutant was degraded in only 90 min. In the absence of UV light, only 10% of methylparaben was removed. An interesting aspect of this work was the study of toxicity carried out by cress seed, showing an inhibition of only 1.09% in the growing of roots, which demonstrated the low toxicity of the products of degradation.

The combination of photocatalytic activity and oxidizing power of H_2O_2 was also applied for the degradation of tetrabromobisphenol A (TBBPA) with a graphene-$BiFeO_3$ composite as catalyst [81]. The catalytic activity was influenced by calcination temperature, pH, presence or not of EDTA, dosage of H_2O_2 and load of catalyst. The degradation of TBBPA approximately followed a kinetics of pseudo first order. Under the most favourable conditions and in the presence of EDTA the rate constant of TBBPA degradation with the graphene-$BiFeO_3$ was 5.43 times higher than that of $BiFeO_3$ and 80% of TBBPA was removed in 15 min. This enhancement in the catalytic activity was attributed to the increasing of the adsorption capacity (due to a large surface area) and to the high electron transfer ability of graphene in the composite, which favoured the generation of reactive species. The composite was stable and could be reused for five cycles without loss of catalytic activity.

3.3. Catalytic Wet Peroxide Oxidation (H_2O_2/Catalyst/Air)

Catalytic wet peroxide oxidation (CWPO) processes are based on the degradation of contaminants by the combined action of a solid catalyst, hydrogen peroxide and air in aqueous solution. In a certain extent, they are similar to Fenton-like processes, because they use H_2O_2 as oxidant; however CWPO processes are carried out in the presence of a flow of air or under pressurized air. They can work with high oxidation efficiency in a wide range of pH without leaching or production of sludge.

Apart from Fenton-type catalysts, including zeolitic materials or composite metal oxides, a reduced number of perovskites has also been tested for CWPO applications. It is important to note that very little theoretical and experimental information is available and there are only a few examples of CWPO using perovskites as heterogeneous catalysts.

The first application of a perovskite in CWPO was carried out by Ovejero et al. [85], who compared the activity of $LaTi_{0.45}Cu_{0.55}O_3$ with that of other catalysts containing Fe or Cu in the degradation of phenol. The reactions were carried out at 100 °C in a system pressurized with air at 1 MPa. The perovskite led to a complete elimination of phenol and a TOC removal of 92% in 45 min. The leaching of copper was 22%; however it was significantly lower than the leaching measured for other catalysts (between 64 and 74%). Considering the fact of the high stability of copper ions in perovskite structures, it is probable that most of the leached copper proceeded from La_2CuO_4 oxide, phase detected by XRD together with the perovskite phase. $LaTi_{0.45}Cu_{0.55}O_3$ was reused in a second cycle, the TOC removal decreasing only to 90%.

Three years later, the same authors extended the study of the CWPO degradation of phenol to other perovskites, in order to elucidate the influence of different reaction conditions (temperature, H_2O_2 peroxide concentration, catalyst concentration and air pressure) on the performance [86]. Three perovskites of $LaTi_{1-x}Cu_xO_3$ composition, with different substitution degree, were tested in the reaction. TOC removal values comprised between 88 and 94% were achieved at 100 °C under air pressure (1 MPa) and stoichiometric amount of H_2O_2 after 2 h. The temperature exerted a significant effect on the activity and only a 15% of TOC removal was reached when reaction was developed at 40 °C. The catalysts could be easily regenerated by calcination in air, leading to similar activity in the second run.

Less drastic operation conditions that the reported above were applied by Faye et al. [87] for the degradation of the same contaminant, phenol, by the action of several $LaFeO_3$ perovskites, synthesized by self-combustion method by varying the glycine/NO_3^- molar ratio. Thus, authors used a flow of air at atmospheric pressure and mild temperatures, 25 or 40 °C. Depending on synthesis conditions, strong differences in the structural, textural and reducibility characteristics were observed. The perovskite having the highest surface area exhibited the highest TOC abatement (76%) and very low iron leaching

(0.27 wt%) after 4 h of reaction at 40 °C. The perovskites were better catalysts than Fe_2O_3, for which a TOC removal of only 10% was reached after 4 h.

4. Processes Based on Peroxymonosulfate

4.1. Peroxymonosulfate Activated by Perovskites (PMS/catalyst)

The peroxymonosulfate ion (PMS) can be considered as a derivate of hydrogen peroxide by replacing one H-atom by a SO_3^- and is stable as triple potassium salt ($2KHSO_5 \cdot KHSO_4 \cdot K_2SO_4$), known by the commercial names of Oxone (from DuPont) and Caroat (from Evonik). PMS is quite stable in water solution and over a wide pH range and shows great potential for generating both sulphate and hydroxyl radicals. Sulphate radicals have a higher half-life than hydroxyl radicals (30–40 ls vs. 20 ns) and they are more selective to react with organics containing unsaturated bonds or aromatic rings during electron transfer, having some operation advantages. Recently, a review of AOPs based on sulphate radicals generated from PMS and persulfate has been published [88]. PMS in an unsymmetrical oxidant that, in the absence of any activator, can partially oxidize some organic compounds according to the redox potential of 1.82 V of reaction (Equation (20)).

$$HSO_5^- + 2H^+ + 2\,e^- \rightarrow HSO_4^- + H_2O \quad (20)$$

In order to generate sulphate radical, the decomposition of PMS must be carried out in presence of an activator, such as transition metals, ultraviolet irradiation (UV), microwave (MW), ultrasound (US), electron conduction and homogeneous and heterogeneous catalysts. The different methods for activation of PMS as well as their application for the removal or persistent organics have been recently revised by Ghanbari et al. [89]. Several nanostructured oxides and carbon materials have been tested as heterogeneous catalysts for PMS activation [90,91]. In spite of the high reactivity of nanostructured oxides, their low recyclability is a problem to be solved. Carbon materials show in general low activities and stabilities. Among heterogeneous catalysts used for PMS activation, materials based on cobalt play an important role. Thus, cobalt oxides, Co-metal oxide and Co-carbon-based supports have been applied for the degradation of different pollutants in presence of PMS. The mechanism for oxidation of organics by Co-assisted decomposition of PMS has been proposed as follows [92–94]:

$$Co^{2+} + HSO_5^- \rightarrow Co^{3+} + SO_4\bullet^- + OH^- \quad (21)$$

$$Co^{2+} + H_2O \rightarrow CoOH^+ + H^+ \quad (22)$$

$$CoOH^+ + HSO_5^- \rightarrow SO_4\bullet^- + CoO^+ + H_2O \quad (23)$$

$$CoO^+ + 2H^+ \rightarrow Co^{3+} + H_2O \quad (24)$$

$$Co^{3+} + HSO_5^- \rightarrow Co^{2+} + SO_5\bullet^- + H^+ \quad (25)$$

$$Co^{2+} + SO_4\bullet^- \rightarrow Co^{3+} + SO_4^{2-} \quad (26)$$

$$SO_4\bullet^- + OH^- \rightarrow SO_4^{2-} + HO\bullet \quad (27)$$

$$SO_4\bullet^- (SO_5\bullet^-, HO\bullet) + \text{organics} \rightarrow \ldots .. \rightarrow CO_2 + H_2O \quad (28)$$

Therefore, three types of reactive radicals including sulphate ($SO_4\bullet^-$), peroxy-sulphate ($SO_5\bullet^-$) and hydroxyl radicals HO• can be generated during PMS activation by cobalt, although peroxy-sulphate radical is less efficient to attack the organic compounds due to its weak oxidizing ability ($E(SO_5\bullet^- / SO_4^{2-}) = 1.1$ V).

Transition mixed metal spinels, iron-based heterogeneous catalysts and other transition metal oxides have also been studied in this system [89]. However, the use of perovskites for activation of PMS has not been revised. In the present review we show some examples of the application of oxide-like perovskites as activators of PMS for the degradation of organics in waters (Table 2).

Table 2. Degradation of pollutants by the combination of peroxymonosulfate (PMS) and oxides type perovskite.

			Concentration			Treatment Efficiency	
Reference	**Catalyst**	**Target Pollutant**	**Catalyst**	**Pollutant**	**PMS**	**Degradation**	**TOC Removal**
[95]	$ACoO_3$ (A = La, Ba, Sr and Ce)	phenol	0.2 g/L	20 mg/L	0.1 mM	95% in 180 min ($LaCoO_3$ and $SrCoO_3$) 80% in 180 min ($BaCoO_3$ and $CeCoO_3$)	81% in 6 h ($LaCoO_3$ and $SrCoO_3$) 35% in 6 h ($BaCoO_3$ and $CeCoO_3$)
[96]	$PrBaCo_2O_{5+\delta}$	phenol, MB	0.1 g/L (for phenol) 0.05 g/L (for MB)	20 mg/L phenol10 mg/L MB	21.2 mM (for phenol) 2.3 mM (for MB)	100% phenol in 30 min 100% MB in 15 min	39.3% at pH 2, 82% at pH 9
[97]	$LaCoO_3/ZrO_2$	RhB	0.1 g/L	10 mg/L	0.1 g/L	100% in 60 min	-
[98]	$SrCo_{1-x}Ti_xO_{3-\delta}$ (SCTx, x = 0.1, 0.2, 0.4, 0.6)	phenol	0.1 g/L	20 mg/L	11.9 mM	85% in 15 min for $SCT_{0.4}$	76.2% in 2 h
[99]	$Ba_{0.5}Sr_{0.5}Co_{0.8}Fe_{0.2}O_{3-\delta}$ (BSCF)	phenol	0.1 g/L	20 mg/L	6.5 mM	100% in 30 min	-
[100]	$LaCo_{0.4}Cu_{0.6}O_3$	phenol	0.1 g/L	20 mg/L	0.65 mM	100% in 12 min	-
[101]	$LaCo_{1-x}Mn_xO_{3+\delta}$ (LCM, x = 0, 0.3, 0.5, 0.7 and 1.0)	phenol	0.1 g/L	20 mg/L	3.25 mM	100% in 20 min for $LaCoO_{3.002}$ 100% in 40 min for $LaCo_{0.5}Mn_{0.5}O_{3.053}$	67% in 40 min
[102]	$LaCoO_3$ (LCO) LCO-SiO_2, CTAB-LCO	PBSA	0.5 g/L	5 mg/L	5 mM	100% in 30 min (LCO-SiO_2) 100% in 5 min (LCO and CTAB-LCO)	-
[103]	$LaCoO_3$	four herbicides (metazachlor, tembotrione, tritosufuron and ethofumesate)	0.5 g/L	1 mg/L (each)	0.1 mM	95% metazachlor, 85% tembotrione, 5% tritosufuron; 45% ethofumesate t = 60 min; pH = 7	-
[104]	$LaMO_3$ (M = Fe, Ni, Cu, Co)	RhB	0.1 g/L	10 mg/L	0.6 mM	42% in 60 min ($LaFeO_3$) 60% in 60 min ($LaNiO_3$) 45% in 60 min ($CuFeO_3$) 98% in 60 min ($LaFeO_3$)	-
[105]	$LaFeO_3$	diclofenac	0.6 g/L	0.15 mM	0.3 mM	100% in 1 h	50% in 2 h

Table 2. *Cont.*

			Concentration			Treatment Efficiency	
Reference	**Catalyst**	**Target Pollutant**	**Catalyst**	**Pollutant**	**PMS**	**Degradation**	**TOC Removal**
[107]	$BiFeO_3$ + visible light	RhB	1 g/L	5 mg/L	5 mM	63% in 40 min (25 °C) 93% in 40 min (45 °C)	-
[108]	$LaCoO_3$-TiO_2 (Co:Ti = 0:1–1:0) + UVA light	four herbicides: metazachlor, tembotrione, tritosufuron and ethofumesate	0.5 g/L	1 mg/L (each)	0.1 mM	90% metazachlor, 97% tembotrione, 20% tritosufuron; 70% ethofumesate t = 60 min; pH = 7	-
[109]	Sr_2CoFeO_6 + UV light	bisphenol F	0.3 g/L	20 mg/L	0.1 mM	75% in 2 h	90% in 6 h

MB: Methylene Blue; PBSA: 2-phenyl-5-sulfobenzimidazole acid; RhB: Rhodamine B; Rh6G: Rhodamine 6G.

As cobalt is catalogued as one of the best transition metals in the homogeneous activation of PMS, most of the described examples for the heterogeneous activation by perovskites are based on those containing cobalt in B position, alone [95–97] or partially substituted by other cations [98–101]. And as occurred in the Fenton-like reactions, phenol is again one of the most studied pollutant [95,96,98–101].

A series of cobalt-perovskite catalysts, $ACoO_3$ (A = La, Ba, Sr and Ce) was tested by Hammouda et al. [95] in the degradation of phenol by action of PMS. $LaCoO_3$ and $SrCoO_3$ showed the best catalytic performance, leading to a depletion of 95% of phenol in 3 h and a TOC removal of 65% in 6 h, in contrast to the 80% of removed phenol and 35% of mineralization degree reached with $BaCoO_3$ and $CeCoO_3$. Phenol degradation followed the pseudo first order kinetics and the intermediate formed were identified as catechol, hydroquinone and benzoquinone. Only between 7 and 12% of phenol was removed by physical adsorption. The activity was not related to the textural properties but to the content of cobalt of samples, the removal of phenol increasing with cobalt amount. The degradation of phenol by PMS in absence of perovskite was only of 10% after 3 h, which indicated the low oxidation power of PMS as compared to sulphate radicals formed in the presence of catalyst.

Su et al. [96] found that both hydroxyl and sulphate radicals were responsible for the degradation of phenol and methylene blue (MB) in the presence of PMS and a mixed ionic−electronic conducting (MIEC) double perovskite, $PrBaCo_2O_{5+\delta}$ (PBC) over a wide pH range, although the sulphate were the major radicals for promoting the degradation of organics. In addition, the oxygen vacancies in perovskite structure played a key role in the activation of PMS and in facilitating easier valence-state changes of the cobalt ions. The PBC catalysed the phenol oxidation with a TOF that was ~196-fold higher than that of the classical Co_3O_4 spinel and 100% phenol was removed in 30 min. In the case of MB only 15 min were necessary to produce the complete degradation.

Zirconia-supported $LaCoO_3$ perovskite, $LaCoO_3/ZrO_2$ and its corresponding $LaCoO_3$ powder, were used to degrade RhB in the presence of PMS [97]. The nanocomposite showed a much higher catalytic activity than $LaCoO_3$ to activate PMS, in spite of the fact that it contained only 12.5 wt% of $LaCoO_3$. RhB was completely degraded in only 60 min and the nanocomposite could be reused for several cycles without activity loss.

Different perovskites of cobalt in B position partially substituted by Ti, Fe, Cu or Mn have been tested in the degradation of phenol [98–101]. In this sense, $SrCo_{1-x}Ti_xO_{3-\delta}$ (SCTx, x = 0.1, 0.2, 0.4, 0.6) perovskites exhibited an excellent activity for phenol degradation under a wide pH range, leading to a faster oxidation than Co_3O_4 and TiO_2 [98]. The order of activity was SCT0.2 ≈ SCT0.1 > SCT0.4 > SCT0.6, therefore the rate of phenol oxidation decreasing with the content of cobalt. The effects of operating conditions and initial pH on the catalytic activity were studied for the SCT0.4/PMS system. At pH ≥ 7 the catalyst led to an optimized performance in terms of higher TOC removal, minimum Co leaching and good catalytic stability, which can overcome the common problems of Fenton reaction and provide a promising application for real wastewater treatments under neutral or alkaline conditions. Less than 5% of phenol was removed by adsorption during the 90 min period and the same amount was degraded by PMS in 90 min in the absence of catalyst.

$Ba_{0.5}Sr_{0.5}Co_{0.8}Fe_{0.2}O_{3-\delta}$ (BSCF) perovskite was very effective for PMS activation to produce free radicals and the subsequent degradation of phenol [99]. On the contrary, it was not active in the production of radicals from activation of other peroxides, such as H_2O_2 or peroxydisulfate (PDS). Authors found that the oxygen vacancies and the metal ions in A position with a less electronegativity than cobalt in the perovskite structure play a key role by conferring cobalt sites a high charge density for interacting with PMS via a rapid charge transfer process and to produce free radicals, resulting in a higher activity when compared to a Co_3O_4 spinel. Thus, 100% of phenol was removed in 30 min with BSCF, in contrast to the 45% of degradation reached with Co_3O_4. Authors concluded that the PMS activation by BSCF gave rise to the generation of both hydroxyl and sulphate radicals.

$LaCo_{1-x}Cu_xO_3$ (x = 0–1) perovskites prepared via sol-gel method with citric acid as organic complexing agent were also tested in the PMS-phenol system [100]. $LaCo_{0.4}Cu_{0.6}O_3$ was the best catalyst, showing a removal efficiency of 100% in only 12 min and a TOF value of 1 h^{-1}, which

was 2.5 times higher than that obtained by Duan et al. (0.4 h^{-1}) [99] for the same concentrations of catalyst and pollutant, although the PMS dosage used in the first case was ten times lower. No significant change on surface of the catalyst was observed after the oxidation reaction, proving the high stability of $LaCo_{0.4}Cu_{0.6}O_3$, although an activity loss of 20% was produced after fourth cycle, due to the poisoning of active sites by adsorption of degradation intermediates. The redox species involved in the mechanism were not only the Co^{2+}/Co^{3+} pair but also the Cu^{+}/Cu^{2+} couple, which reacted with both $SO_4\bullet^-$ and HO•.

Miao 2018 [101] synthesized a series of $LaCo_{1-x}Mn_xO_{3+\delta}$ (LCM, x = 0, 0.3, 0.5, 0.7 and 1.0) perovskites, calcined at different temperatures, showing over stoichiometric oxygen. Authors found that the interstitial oxygen plays a key role in the catalytic activity for degradation of phenol, in such way that a proper amount of interstitial oxygen promotes the electron transfer rate of the perovskite but an excess hinders this process. The most active catalyst was that containing only cobalt in B position, that is, $LaCoO_3$, which led to a complete depletion of phenol in only 20 min. Among all the substituted catalysts, $LaCo_{0.5}Mn_{0.5}O_{3.053}$, calcined at 900 °C, exhibited the best performance, due to its high interstitial oxygen ion diffusion rate. Furthermore, its stronger relative acidity contributed to an enhanced stability. Phenol was completely degraded with this catalyst after 40 min. Considering that manganese ions are much cheaper and less toxic than cobalt ions, these substituted perovskites are an appropriate alternative for the activation of PMS.

$LaCoO_3$ perovskite has proved to be very efficient for the activation of PMS in the degradation of different organic pollutants [102–104]. The degradations of aqueous solutions of 2-phenyl-5-sulfobenzimidazole acid (PBSA) using PMS activated with $LaCoO_3$ perovskites prepared by three different methods was investigated by Pang et al. [102]. $LaCoO_3$ was prepared by a normal precipitate method (sample named as LCO), by introduction of cetyltrimethylammonium bromide (CTAB-LCO) and by a hydrothermal method with the adding of silicon (LCO-SiO_2). LCO-SiO_2 was active in a wider pH range (4–8), leading to a complete removal of PBSA in 30 min and showing a very low leaching of metal ions. On the contrary, LCO and CTAB-LCO presented a contribution of the homogeneous reaction to the total activity, due to the leached metals, which resulted in the PBSA depletion of 100% in only 5 min. From studies with radical quenchers and from identified intermediates authors concluded that for LCO-SiO_2 the activation of PMS resulted from the combination of $SO_4\bullet^-$ and electronic transfer reaction. However, in the case of LCO and CTAB-LCO, both $SO_4\bullet^-$ and HO• radicals were involved.

More recently, Solís et al. [103] have reported the combination of $LaCoO_3$ and PMS for the removal of various aqueous herbicides (metazachlor, tembotrione, tritosufuron and ethofumesate). The catalyst amount exerted a positive influence on herbicides conversion, which increased when the load of catalyst did from 0.5 to 1.5 g/L. An increment in the pH values reduced cobalt leaching and decreased PMS depletion. As the point of zero charge (PZC) value of $LaCoO_3$ was 9.08, at acidic or neutral pH the catalyst surface is positively charged and as a result it interacts more easily with the anions from PMS. With respect to the influence of PMS concentrations, those equal or above 0.5 mM produced the instantaneous removal of metazachlor, tembotrione and ethofumesate while tritosulfuron required almost one hour to be completely degraded when 0.5 mM of PMS was used.

The high activity of cobalt ions for PMS activation was confirmed by Lin et al. [104], who tested a series of $LaMO_3$ perovskites (M=Co, Cu, Fe and Ni) in the removal of RhB. Once more, $LaCoO_3$ was the most active, followed by $LaNiO_3$, $LaCuO_3$ and $LaFeO_3$. The mechanism of reaction was studied by addition of different scavengers or radical inhibitors. Authors found that both Co^{3+}/Co^{2+} and La^{3+}/La^{4+} ions decomposed PMS yielding mainly sulphate radicals and hydroxyl radicals in lesser extent. By comparison of the obtained rate constants with other from literature, authors concluded that $LaNiO_3$, $LaCuO_3$ and $LaFeO_3$ were no competitive with other existing catalysts, because of the low activity of Ni, Cu and Fe for PMS activation, in contrast to $LaCoO_3$, which exhibited a rate constant comparable or even higher than those reported for other catalysts.

Iron in B position of perovskites has resulted to be also an efficient cation for the PMS activation [105,106]. The oxidative degradation of diclofenac (DCF), a non-steroidal anti-inflammatory drug, was carried out in the presence of $LaFeO_3$ and PMS [105]. DFT studies allowed authors to conclude that a strong interaction occurs between the Fe (III) sites on $LaFeO_3$ surface and PMS, with the formation of an inner-sphere complex and the transfer of electrons from PMS to Fe (III). Sulphate radicals were identified as the major responsible for DCF degradation by the $LaFeO_3$ /PMS system. Although 100% of DCF was removed in only 1 h, the mineralization was only of 50% and fifteen different intermediates were formed.

$La_{0.8}Ca_{0.2}Fe_{0.94}O_{3-\delta}$ and Ag-$La_{0.8}Ca_{0.2}Fe_{0.94}O_{3-\delta}$ were tested by Chu et al. [106] in the removal of phenol, MB and rhodamine 6G. From electrochemical impedance spectra, authors concluded that Ag nanoparticles and lattice oxygen vacancies improve the p-type conductivity of the perovskite. Furthermore, the O_2 of solution is adsorbed on the oxygen vacancies and as a consequence, in order to replace the lost oxygen, more $SO_5\bullet^-$ react generating more sulphate radicals. Under the optimum conditions, around 84–90% of MB was degraded in only 45 min. When using Ag-$La_{0.8}Ca_{0.2}Fe_{0.94}O_{3-\delta}$ rhodamine 6G and phenol were completely removed in 15 and 10 min, respectively. This perovskite was also very efficient for the removal of *Escherichia coli*.

4.2. Peroxymonosulfate Activated by the Combination of Perovskites and Light Irradiation (PMS/Catalyst/Light)

The combination of PMS activation by a perovskite and light irradiation has been applied for the degradation of different pollutants [107–109]. Rhodamine B (RhB) was used as model of organic pollutant for studying the PMS activation by a $BiFeO_3$ microsphere in presence of visible light [107]. To confirm the contribution of the oxidizing radical species, ethanol (EtOH), t-butanol (t-BuOH) and 1,4-benzoquinone (BQ) were employed as radical scavengers. The results indicate that the main generated radical species during the activation of PMS by $BiFeO_3$ were HO• and $SO_4\bullet^-$ radicals. However, the $O_2\bullet^-$ radicals, which are formed at longer reaction times, also play an important role in the degradation of RhB. Authors explained the reaction mechanism as follows. $BiFeO_3$, with narrow band gap energy (1.92 eV), can be easily excited by visible light and the electrons and holes generated by action of light can react with Fe^{3+} and RhB, respectively. Simultaneously, Fe^{3+} and Fe^{2+} can also activate PMS to yield $SO_4\bullet^-$ and $SO_5\bullet^-$ radicals, which degrades RhB. About 63% of RhB was degraded in 40 min by $BiFeO_3$/PMS/vis light system, in contrast to 43% of removal in the absence of perovskite. The catalyst was used in three consecutive cycle runs without significant loss of photocatalytic activity.

The combination of a cobalt perovskite ($LaCoO_3$) with a photocatalyst (TiO_2) in different molar ratios (Co:Ti = 0:1–1:0) was used to activate PMS for the oxidation of a mixture of four herbicides (metazachlor, tembotrione, tritosulfuron and ethofumesate) [108]. Same authors had previously tested $LaCoO_3$/PMS system for the degradation of the same herbicides [103]. In general, $LaCoO_3$-TiO_2 with Co:Ti ratios in the range 0.1:1 to 0.5:1 showed a higher activity than the rest of solids tested, although a Co/Ti ratio of 0.1:1 was enough to reach enhanced degradation rates when compared to pristine titania or pure perovskite. The number of degraded herbicides by $LaCoO_3$-TiO_2/PMS system was 3.5–5 times higher in the presence of UVA-light and the reaction followed a second order kinetic, depending of concentration of both PMS and herbicides. As complete mineralization was not achieved, authors carried out studies to assess the potential phytotoxicity of the accumulated intermediates, concluding that all samples did show no phytotoxicity after 180 min of treatment for PMS concentrations $\geq$ 0.15 mM.

A double cobalt perovskite, Sr_2CoFeO_6, was tested in the mineralization of bisphenol F (BPF) in neutral medium by activation of PMS under UV irradiation [109]. Neither direct UV photolysis nor PMS alone degraded the BPF and Sr_2CoFeO_6 exhibited higher activity (75% of BPF degradation in 2 h) than the corresponding single perovskites, $SrCoO_3$ (60%) and $SrFeO_3$ (35%), caused probably by an accelerated reduction of Fe^{3+} in the presence of cobalt ions. UV irradiation also improved the

mineralization degree of BPF and values of TOC removal in 6 h increased from 65% to 90% when Sr_2CoFeO_6/PMS system was irradiated. As a novel aspect of this work, authors studied the influence of chemicals co-existing in the natural water matrix, such as humic acid and inorganic anions (Cl^-, HCO_3^- and CO_3^{2-}), on the inhibition of degradation of bisphenol.

5. Photocatalytic Oxidation (Light/catalyst)

Within AOPs, photocatalyst-based degradation methods represent an interesting research field where there has been continuous development. Heterogeneous photocatalysis is widely recognized as an effective technology for treating waters containing some refractory organic compounds through the photogeneration of oxidizing radicals such as HO• and O^{2-}•. It is a green technology with broader application prospect and compared with the traditional chemical oxidation, photocatalysis is usually non-toxic, non-corrosive and harmless to the environment. The photocatalytic oxidation is based on the use of a semiconductor and ultraviolet-visible (UV-vis) radiation (see Figure 4). The fundamental step of the process is generation of electron-hole pairs, which requires absorption of photons with adequate energy and promotion of electrons from the valence band to the conduction band. The photogenerated charge carriers participate in a series of reactions producing highly reactive radicals. One of the most relevant applications of this technique is the degradation of environmental pollutants in aqueous wastewater into less harmful products. These treatments are very appropriate because of their on-place use and because they do not have extra energy consumption. The degradation of organics is normally accomplished of semiconductors such as zinc oxide (ZnO) or titanium dioxide (TiO_2). The latter is currently the most popular photocatalyst due mainly to its specific photocatalytic properties like for example strong oxidizing power, high chemical stability and relative inexpensiveness. Recently, different photocatalytic materials capable of efficiently working with sunlight, based mostly on TiO_2 and their combination with solar collectors, have been revised [110].

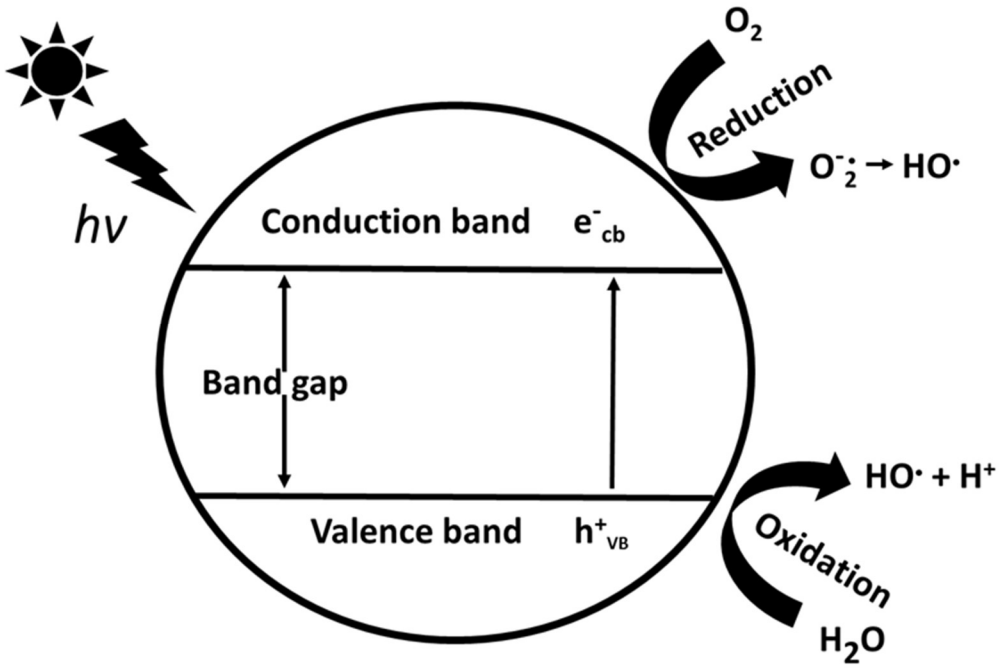

Figure 4. Schematic illustration of a model photocatalytic system showing the contribution of hole-electron couples to the formation of radicals.

Unfortunately, the use of TiO_2 catalysts is limited by the large band gap of TiO_2 (Eg = 3.2 eV), being active only under UV light. Considering that the sunlight is composed mainly of visible light (43%) while only 4% of the spectrum is UV light, visible-light photocatalytic performance is desirable in order to effectively utilize the sunlight. In this sense, considerable effort is being devoted to developing

alternative heterogeneous photocatalysts, which are active under visible light. Among the various materials, some perovskites have been considered as a promising photocatalysts, since they present high activity in the long band of visible-light. They can be used alone or combined with TiO_2 in form of composites, with the aim of narrowing the bandgap of this oxide.

One of the perovskites more widely studied as photocatalyst is $LaFeO_3$ [111–122], due to its narrow band gap (often less than 3.0 eV), which can be excited easily under visible light or UV light irradiation. It can be used auto supported or in form of composites and rhodamine B (RhB) has been tested by different authors as model molecule in the evaluation of its photocatalytic activity [111,112,114,119–122].

In Reference [111] $LaFeO_3$ particles prepared by sol-gel method were able to degrade RhB in 24% under visible irradiation, showing a higher activity than that of international P-25TiO_2. Authors found a reverse correlation between crystallite size and photocatalytic activity, the most active sample being that exhibiting the smallest size. Values of degradation comprised between 15 and 50% were reached when $LaFeO_3$ nanoparticles were prepared by using silica SBA-16 as template [112]. The high surface area and crystallinity of samples were responsible for the adsorption and photocatalytic degradation of RhB, respectively.

Li et al. [114] prepared different samples containing $LnFeO_3$ (Ln = La, Sm) nanoparticles by sol–gel method at different calcination temperatures. 80% of RhB was degraded in 2 h by $LaFeO_3$ under visible light, in contrast to the 20% obtained with $SmFeO_3$. When H_2O_2 was added to the reaction media, the photocatalytic activity improved due to the synergistic effect between the semiconductor photocatalysis and Fenton-like reaction. Complete degradation of RhB was achieved after 3 h of reaction when microspheres composed of perovskite $LaFeO_3$ nanoparticles, prepared by hydrothermal method, were used as photocatalysts [119]. In this case, the hydrothermal reaction conditions and the concentration of citric acid played an essential role in the development of $LaFeO_3$ microspheres. The efficiency of $LaFeO_3$ microspheres was higher than that of $LaFeO_3$ prepared by microwave assisted method [120] (95% of degradation of RhB in 3 h).

As an alternative way to obtain perovskite-type nanoparticles, graphitic carbon nitride (g-C_3N_4) has been combined with $LaFeO_3$ by using a solvothermal method [121] according to the scheme of preparation shown in Figure 5. The synergistic interaction between $LaFeO_3$ and g-C_3N_4 improved the separation efficiency of photogenerated electron-hole pairs. Then the photocatalytic activity for the degradation of RhB was 19 times higher than that of $LaFeO_3$ under visible light irradiation. In addition, the catalysts kept excellent stability after four cycles.

Figure 5. Schematic illustrating the synthesis of the $LaFeO_3$/g-C_3N_4 heterojunction. With permission from [121].

To achieve more homogeneous $LaFeO_3$ nanoparticles, Ren et al. [122] used reduced graphene oxide as template. They obtained nanoparticles anchored on graphene oxide by combining the sol-gel method and high-temperature annealing. The $LaFeO_3$–rGO can work under visible-light irradiation as an efficient catalyst for the degradation of RhB and MB, the bandgap of $LaFeO_3$ nanoparticles on

reduced graphene oxide being of 1.86 eV. The oxidation process was dominated by the electron transfer since the presence of rGO facilitated the electron-hole separation.

Methylene blue (MB) has been degraded under the photocatalytic reactions with $LaFeO_3$ perovskites [116,117] and $LaFeO_3$ doped in A position [115,118], whose activity is strongly influenced by the process of synthesis. There are many methods to prepare $LaFeO_3$ such as sol-gel, co-precipitation, electro-spinning, citric acid complex, stearic acid solution combustion or glycine combustion at high temperature. Among these methods, the sol-gel process has been proven to be one of the most effective [116] and MB and methyl orange were completely degraded after visible light irradiation for 4 h of $LaFeO_3$ synthesized by sol-gel method and calcined under vacuum microwave. The photodegradation process of MB on $LaFeO_3$ followed a pseudo-first-order kinetic process.

However, sol-gel method and solid-state reactions need annealing at a high temperature which results in short homogeneity and high porosity of the samples without control on the particle size. As an alternative way, the microwave assisted synthesis allows preparing nanoparticles with small size, narrow size distribution and high reactive ability in a time-saving process. In this regard, $LaFeO_3$ with high crystallinity and sphere-like shape was able to decolorize a MB aqueous solution in only 90 min of exposure to visible light [117].

A strategy to improve the photocatalytic efficiency of perovskites is by doping in A position [115,118]. Thus, a series of $LaFeO_3$ perovskites doped with Li, $La_{1-x}Li_xFeO_3$ (with x = 0, 3, 5 and 7%) were active under light irradiation for the degradation of MB and arcylon effluents, $La_{0.97}Li_{0.03}FeO_3$ showing the highest activity [115]. $LaFeO_3$ and Ca-doped $LaFeO_3$, synthesized via reverse microemulsion without additional high temperature calcination process [118] were active in the photocatalytic degradation of MB under the action of visible light. When $La_{0.9}Ca_{0.1}FeO_3$ was used instead of $LaFeO_3$, the degradation rate of MB improved 30%.

$LaFeO_3$ and its corresponding double perovskite, La_2FeTiO_6, have also been tested in the degradation of p-chlorophenol [113] under visible light. Authors correlated the photocatalytic activity with differences in structure or surfaces properties. Thus, the optical property in the visible light region and the inferior symmetry at the Fe nucleus of La_2FeTiO_6 resulted in a better performance with respect to that of $LaFeO_3$.

Apart from $LaFeO_3$ other perovskites have been used as photocatalysts. In this regard, the fact that $LaCoO_3$ hollow nanospheres exhibit a band gap of 2.07 eV makes this compound a promising candidate material for photocatalytic applications. Fu et al. [123] studied the photocatalytic degradation of MB, methyl orange and neutral red under UV irradiation. UV–vis analysis showed that $LaCoO_3$ hollow nanospheres exhibited excellent photocatalytic activity, reaching degradation values near 90% in 100 min for the three contaminants. Moreover, the authors discussed the influence of temperature and time of calcination on the structures of $LaCoO_3$ and its formation mechanism.

Alkali earth titanates, such as $SrTiO_3$, are perovskite-type oxides based on a Ti-O polyhedron, showing a similar energy band structure to that of TiO_2. Furthermore, $SrTiO_3$ shows a wide absorption band in the ultraviolet region in the 300–400 nm range. As a result it can be used as photocatalyst, whose activity can be improved by incorporation of CeO_2 to the structure, which shows strong UV absorption in the 300–450 nm range. In this sense, a $SrTiO_3/CeO_2$ composite was used in the photodegradation of two azo dyes, C.I. Reactive Black 5 [124] and C.I. Direct Red 23 [125]. The influence of pH on the photoactivity was studied in the first case. Authors extended the study to the influence of other parameters, such as catalyst dose, concentration of dye, pH value, irradiation intensity and use of KI as scavengers, in the second one. Under the optimum conditions, a complete degradation of C.I. reactive black 5 and C.I. direct red 23 was achieved in 120 min and 60 min, respectively. Authors proposed a tentative degradation pathway based on the sensitization mechanism of photocatalysis.

Recently, bismuth-based perovskites have also attracted interest as photocatalysts due to their particular electronic structure that reduces the charge mobility and the band gap to ~2 eV [126–129]. $BaBiO_3$ powders with a base centred monoclinic structure exhibited good activity for the water-splitting reaction and the degradation of rhodamine B dye under visible light [126]. Authors demonstrated

that the catalytic activity strongly depended on the crystallinity of the materials, $BaBiO_3$ prepared by solid state being the catalyst with the highest crystallinity, the lowest resistance to the charge transfer and the greatest photocatalytic performance. Another bismuthate, $KBiO_3$, was investigated as a visible-light-driven photocatalyst in the degradation of organic pollutants, such as RhB, crystal violet, MB and phenol [127]. The difference between the degradation mechanisms of these organic pollutants under the action of $KBiO_3$ depended on competition of the photocatalysis, redox reaction and adsorption mechanisms. In the case of RhB and crystal violet, the redox potentials are higher than that of $KBiO_3$ (1.59 eV) but lower than its band gap energy (2.04 eV), thus only the adsorption and photooxidation controlled the reactions. MB presents a redox potential lower than the band gap of $KBiO_3$ and in this case the reaction was controlled by both the photooxidation and chemical oxidation. In the case of phenol, photooxidation was observed at the end steps of the process whereas quick adsorption and chemical oxidation were determined at the initial stage. A double Bi-perovskite, $Bi_2Fe_4O_9$, composed of nanoplates, which behaves as a multiband semiconductor [128] was tested in the photocatalytic oxidation to aqueous ammonia oxidation and phenol under visible light irradiation. The catalyst displayed a higher activity when compared to its bulk material. The improvement of photocatalytic performance of $Bi_2Fe_4O_9$ could be due to the efficient electron-hole separation that may act as electron-hole recombination centres. The photocatalytic performance for phenol oxidation enhanced when an appropriate amount of, H_2O_2, was added, which can act as a strong electron scavenger and also as a promoter of the Fenton-like reaction.

$LaMnO_3$ perovskite is another promising photocatalyst owing to its catalytic and electrical properties, price, nontoxicity and high stability. However, a high combination rate of electron/hole pairs and the agglomeration of particles are some of the perovskite limitations. Semiconductor coupling with carbon materials is believed to induce cooperative o synergistic interactions retarding the fast recombination of the charge carriers and getting better the photocatalytic activity. In this sense, Huang et al. [130] observed a higher efficiency for photodegradation of acid red C-3GN over a series of $LaMnO_3$-diamond composites than for $LaMnO_3$. In the composites, the perovskite particles are uniformly distributed on the diamond surface creating a network structure, which increases the active sites and the absorption of dye molecules. The composite showed the best photocatalytic activity when the mass ratio was $1LaMnO_3/2$diamond.

AuNP/$KNbO_3$ have shown photocatalytic activity in the photooxidation of sec-phenethyl alcohol to acetophenone under the action of visible light in the presence of H_2O_2 [131]. Photophysical properties of $KNbO_3$ and TiO_2 are fundamentally similar, with band gaps near 3.2 eV; however, the particle size of $KNbO_3$ presents advantages over TiO_2 since small particle size of TiO_2 make difficult its separation from reaction solutions. The activity of this AuNP-decorated $KNbO_3$ was superior to that of undecorated $KNbO_3$.

In recent years most researchers have concentrated their attention on modifying perovskite by doping with a transition metal or non-metal to improve the catalytic activity. The doping allows the recombination of centres of electron-hole pairs in the semiconductor particles. For instance, the doping with C and S atoms improved the photocatalytic activity of $SrTiO_3$ for oxidation of 2-propanol [132], because a new absorption edge in the visible light region was produced.

Several articles report the benefit of using nanostructures to improve the photocatalytic activity with respect to the bulk samples [129,133,134]. Thus, perovskite-type $BiFeO_3$ nanoparticles showed increased degradation ability of methyl orange under visible light irradiation with respect to bulk $BiFeO_3$, probably due to the higher surface area of the nanoparticles [129]. As a result, more than 90% of MO was decolorized after 8 h under UV-vis irradiation and after 16 h under visible light when $BiFeO_3$ nanoparticles were used. In contrast, only 70% of dye was degraded after 16 h by the action of UV-vis light in the presence of bulk $BiFeO_3$. Dong et al. [133] found that $LaCoO_3$ nanofibers prepared at different temperatures presented better photocatalytic activity for the degradation of RhB than $LaCoO_3$ particles. Nanofibers exhibited an increased surface, providing more photocatalytic active sites on the inner/outer surfaces that led to a complete degradation of RhB in only 50 min for the

best catalyst, which resulted to be that with a high degree of crystallinity of $LaCoO_3$ nanofibers and containing some residual carbon. $PrFeO_3$ porous nanotubes showed high optical absorption in the UV-visible region and an energy band gap of 1.97 eV [134], displaying a higher photocatalytic activity in the degradation of RhB than $PrFeO_3$ nanofibers or $PrFeO_3$ nanoparticles. Thus, 46.5% RhB was degraded by the nanotube sample in 6 h, whereas decolorization efficiency was 29.5% and 15.7% for nanofibers and nanoparticle samples, respectively. $PrFeO_3$ nanotubes were used for three cycles of photodegradation, showing a slight deactivation.

Silver orthophosphate (Ag_3PO_4) has been extensively studied due to its good activity as photocatalyst for organic pollutants degradation under the action of visible light [135]. However, the photocorrosion together with the formation of metallic Ag in the surface of catalyst limit the stability and cause a decrease in the activity and reusability. Several strategies have been proposed to improve the photostability of Ag_3PO_4, among them, the synthesis of composites perovskite-type (ABO_3) has attracted considerable attention due to its high catalytic activity. Guo et al. [136] synthesized and characterized several $Ag_3PO_4/LaCoO_3$ composites with different ratios, which were evaluated in the photocatalytic degradation of bisphenol A. For the composite containing 10% of $LaCoO_3$, the contaminant was completely degrader after 40 min, achieving a TOC removal of 77.3%. Furthermore, the authors investigated in detail the degradation intermediates and the photocatalytic mechanism.

It has been also found that by introducing perovskites in a TiO_2 matrix, a beneficial effect in the photocatalytic activity of TiO_2 can be obtained. Thus, Gao et al. [137] synthesized multi-modal TiO_2-$LaFeO_3$ composite films by a two-step method, which exhibited high photocatalytic activity in the degradation of MB aqueous solution (60% of degradation in 1 h). In comparison with TiO_2 and $LaFeO_3$ materials, the composite obtained exhibited good microstructural properties and high specific surface area. The introduction of $LaFeO_3$ not only improved the photocatalytic activity and the hydrophilicity but also influenced the interfacial charge transfer process. The same composite, TiO_2-$LaFeO_3$, was prepared by Dhinesh et al. [138] by a hydrothermal method and tested in the degradation of methyl orange in aqueous solution under visible light irradiations. TiO_2-$LaFeO_3$ composite exhibited enhanced visible light photocatalytic properties in comparison with $LaFeO_3$ nanoparticles due to a synergetic effect.TiO_2 causes the inhibition of the recombination between photoinduced electron and hole pairs and $LaFeO_3$ perovskite played an important role in extending light absorption into the visible region. Halide perovskite $CsPbBr_3/TiO_2$ composites [139] also showed an enhanced activity in the selective oxidation of benzyl alcohol to benzaldehyde under visible light irradiation. Action spectra and electron spin resonance studies showed that photo-excited electrons generated within $CsPbBr_3$ were transferred to the conduction band of TiO_2, forming, via the reduction of oxygen, superoxide radicals. 50% of benzyl alcohol was oxidized after 20 h of irradiation.

Table 3 summarizes the applications of perovskite-like oxides synthesized by different methods as photocatalysts for the degradation of different organics.

Table 3. Oxides type perovskite applied as photocatalysts for the degradation of different organic contaminants in aqueous solution.

Reference	Catalyst	Preparation Procedure	Contaminant	Light (Irradiation Source)
[111]	$LaFeO_3$	Sol–gel	RhB	Visible
[112]	$LaFeO_3$	Sol–gel, SBA-16 as template	RhB	Visible
[114]	$LnFeO_3$ (Ln = La, Sm)	Sol–gel	RhB	Visible
[119]	$LaFeO_3$	Hydrothermal	RhB	Visible
[120]	$ReFeO_3$ microspheres (Re: La, Sm, Eu, Gd)	Microwave	RhB	Visible
[121]	$LaFeO_3$, g-C_3N_4	Solvothermal	RhB	Visible
[122]	$LaFeO_3$-rGO	Sol-gel	MB and RhB	Visible
[116]	$LaFeO_3$	Sol–gel, Microwave	Methyl orange and MB	Visible
[117]	$LaFeO_3$	Microwave	MB	Visible
[115]	Li-doped $LaFeO_3$	Sol-gel	MB and arcylon	UV-visible
[118]	$LaFeO_3$, Ca-doped $LaFeO_3$	Reverse microemulsion	MB	Visible
[113]	$LaFeO_3$, La_2FeTiO_6	Sol–gel	p-Chlorophenol	Visible
[123]	$LaCoO_3$	Surface-ion adsorption	MB, methyl orange and neutral red	UV
[124]	$SrTiO_3/CeO_2$	Dry ($SrCO_3$, CeO_2)-wet (sol-gel $Ti(OC_4H_9)_4$) composition	Reactive black 5	UV
[125]	$SrTiO_3/CeO_2$	Dry ($SrCO_3$, CeO_2)-wet (sol-gel $Ti(OC_4H_9)_4$) composition	Direct Red 23	UV
[126]	$BaBiO_3$	Solid state, hydrothermal	RhB, water splitting	Visible
[127]	$KBiO_3$	Solid phase heating	RhB, crystal violet, MB, phenol	Visible
[128]	$Bi_2Fe_4O_9$	Hydrothermal method	phenol, aqueous ammonia	Visible
[130]	$LaMnO_3$–diamond	Sol-gel	Acid red C	Visible
[131]	Au NP/$KNbO_3$	Deposition/precipitation + thermal reduction	Sec-phenethyl alcohol	Visible
[132]	S, C-co-doped $SrTiO_3$	Calcination	2-Propanol	Visible
[129]	$BiFeO_3$ nanoparticles	Sol-gel	Methyl orange	UV-Visible
[133]	$LaCoO_3$ nanofibres	Electrospinning	RhB	UV
[134]	$PrFeO_3$ (nanotubes, nanofibers, nanoparticles)	Electrospinning, annealing	RhB	Visible
[136]	$Ag_3PO_4/LaCoO_3$	Liquid deposition	Bisphenol	Visible
[137]	$LaFeO_3/TiO_2$	Two-step	MB	Fluorescent
[138]	$LaFeO_3/TiO_2$	Hydrothermal	Methyl orange	Visible
[139]	$CsPbBr_3/TiO_2$	Wet-impregnation	Benzyl Alcohol	Visible

MB: Methylene Blue; RhB: Rhodamine B.

6. Processes under Dark Ambient Conditions

As shown above, to date, great success has been achieved for producing visible-light photocatalysts by doping perovskites or designing composites. Other perovskites have been proven active in AOPS involving an additional chemical oxidant, such as ozone, hydrogen peroxide or peroxymonosulfate. Nevertheless, both kinds of processes using or light or chemical oxidant are expensive, thus limiting their practical applications. Therefore an effort has to be made to find new catalysts capable of working under dark ambient conditions, as potential low-cost alternative for the remediation of waters. A few examples of the application of perovskites for the degradation of organics in waters in dark ambient conditions are shown next.

A layered perovskite La_2NiO_4 crystal [140] can act as a round-the-clock photocatalyst and efficiently degrade phenolic pollutants in the dark. This photocatalyst can produce photoelectrons not only by visible light irradiation but also from some reactant molecules in the dark leading to the degradation of 4-chlorophenol (4-CP). 4-CP^- anions can donate electrons to La_2NiO_4, what is followed by the reaction with dissolved oxygen to generate O_2-• and reaction with H^+ to form HO• radicals, which can oxidize 4-CP• radicals into CO_2. $LaCoO_{3-x}$ (x= 0-0.075) [141] calcined at different temperatures also displayed activity for the degradation of methyl orange in the dark. 17% of dye was removed with the best catalyst in 45 h in the absence of light. The degradation rate improved under the visible light due to the optical property of $LaCoO_{3-x}$, achieving degradation values of 40%. $Sr_{0.85}Ce_{0.15}Fe_{O3-\delta}$ [142] can also work in the dark after thermal activation. $SrFeO_3$ is known as photocatalyst since the bandgap energy values are comprised between 1.80 and 3.75 eV; however, the doping with Ce improves its redox properties and exerts a positive role in oxidation reactions. The catalyst was applied to remove RhB and Orange II from aqueous solution. In the first case the degradation after 7 h only increased from 40 to 60% in the presence of visible light. On the contrary, for the degradation of Orange II it was necessary to irradiate the catalyst, because only 5% was removed in the dark.

Other examples of the use of perovskites as catalysts for degradation of contaminants in aqueous solution in the absence of an oxidant or light have been described. In this regard, methyl orange (MO) was degraded by a layered perovskite, $La_4Ni_3O_{10}$, without additional reagents or external energy [143]. The dye degradation occurred via electrons transfer from the dye molecules to the perovskite and then to the dissolved oxygen, which acted as electrons acceptor. The same dye, MO, was degraded by $LaNiO_{3-\delta}$ under dark ambient conditions (room temperature and atmospheric pressure) [144]. Under the optimum conditions 94.3% of MO was degraded after 4 h. Authors concluded that MO was decomposed by two synergic effects derived from nickel present at the surface of $LaNiO_{3-\delta}$ and the formation of lanthanum carbonate.

$SrFeO_{3-\delta}$ perovskite synthesized by a combined high temperature and high-energy ball milling process was active in the degradation or bisphenol A (BPA) and Acid Orange 8 under dark ambient conditions [145]. The complete degradation of BPA was produced after 24 h, with a TOC removal of 83%. In the case of dye, the full decolorization was attained in only 1 h. By last, more recently, Chen et al. [146] tested a series of $Ca_xSr_{1-x}CuO_{3-\delta}$ (x= 0-1) perovskites in the removal of Orange II dye, widely used in the textile industry. Samples containing a higher amount of Ca were more active for the degradation of Orange II in dark conditions. A depletion in concentration of dye of 80% was reached in only 10 min, which increased to 95% after 1 h. However the mineralization was partial only and some by-products were formed, reaching a TOC removal of 60%. The catalysts were stable after 9 cycles of reusing.

7. Summary and Perspectives

In this paper we have summarized the applications of perovskites as catalysts in heterogeneous advanced oxidation processes for the degradation of pollutants present in waters. Processes have been classified and revised according to the oxidant employed in the process, that is, ozone, hydrogen peroxide and peroxymonosulfate, which can be used alone or combined with light irradiation.

The photocatalytic oxidation, consisting in the activation of a catalyst, in this case, a perovskite, by irradiation with UV or visible light, has also been revised.

The various systems described here using perovskites were shown to effectively degrade and remove specific pollutants from waters. Phenol has been the most studied but other pollutants, such as dyes (especially rhodamine B and methylene blue), phenolic compounds, herbicides and some drugs have also been reported. Although single ozonation (in the absence of catalyst) has been widely used in water and wastewater because is an effective oxidation process, the use of a catalyst improves the decomposition of ozone and the production of hydroxyl radicals and overall increases the degree of mineralization of the contaminants. However, the use of perovskites in this type of processes is very limited and only a few studies have been carried out. Significantly higher is the number of papers related to the application of perovskites in Fenton-like processes, using H_2O_2 as producer of radicals. The stabilization of cations with unusual oxidation states and redox properties in the perovskite network make these oxides good candidates for this type of reaction. Thus, most of reported perovskites contain iron (Fe^{2+}/Fe^{3+}), the Fenton reactant by excellence, in B position but other transition metals, such as copper, manganese or titanium have also been resulted active for the Fenton-like degradation of contaminants. When the H_2O_2/perovskite system is combined with the irradiation of light (photo-Fenton process) the degradation of contaminant and TOC removal generally increase because the rate of production of HO• radicals is higher.

Several examples of perovskites as activators of peroxymonosulfate (PMS) for the production of radicals able to degrade organics present in waters have been presented. It should be remarked that the treatment with PMS is more expensive than other AOPs, due to the price of the reagents. As cobalt is catalogued as one of the best transition metals in the homogeneous activation of PMS, most of the described examples for the heterogeneous activation by perovskites are based on those containing cobalt in B position, alone or substituted by other cations.

It should be pointed that one of the AOPS in which perovskites have been more extensively applied is the heterogeneous photocatalysis, because they present high activity in the long band of visible-light. These processes generally lead to higher TOC removal than processes based on a chemical oxidant. Perovskites have been used in photocatalytic degradation or organics alone or combined with TiO_2 in form of composites, in this way narrowing the bandgap of this oxide. Additionally, the main strategy to improve the photocatalytic activity has been the substitution of the element in A or B position, which leads to the introduction of defects into the narrow band gap and to the formation of oxygen vacancies, which inhibit the recombination between the photogenerated electrons and the holes. Again, as in Fenton-like processes, perovskites containing iron in B position have been the most studied.

Perovskites have resulted been active by alone in the revised AOPs. However, majority of studies were carried out in semi-batch and batch reactors, while continuous fixed bed reactors, which are promising from the practical point of view, have not extensively studied for treatment of real wastewaters. In this sense it can be expected that in the future more studies will be devoted to them.

The low surface area of perovskites implies a limited interaction with the contaminants. In order to increase the surface area, new synthesis methods have been applied and some strategies have been developed, such as their supporting on mesoporous silica supports, honeycombs or the formation of composites. Another strategy to improve catalytic activity of perovskites in AOPs is the hetero-doping in order to produce more active sites of the low-valence B-site transition metals (i.e., Fe^{2+}, Cu^{+} and Ti^{3+}) or to introduce oxygen vacancies, which can facilitate the transformation of H_2O_2 (or PMS) into HO•. Furthermore, the use of nanostructures improves the catalytic behaviour with respect to the bulk samples. Considering all of this, we think that research of forthcoming years will be addressed to design new synthesis methods which allow the obtaining of perovskites in form of nanostructures, nanoparticles or nanofibers and also to search new materials based on perovskites containing other different active cations and exhibiting higher surface areas, which can be extended to the removal of other persistent contaminants present in waters.

By last, it should be remarked the high cost of AOPs, involving light or chemical oxidants, which usually have to been constantly fed to keep the process operative. Recent studies reporting promising results of the application of perovskites for degradation of some organics under dark ambient conditions, should encourage researchers in a short-term future to the search of similar systems capable of degrading other contaminants without necessity of using energy or reagents, which would considerably reduce the cost of the process.

Author Contributions: M.L.R.C. chose the topic and designed the organization of paper; M.L.R.C. and E.C. performed the literature search and wrote the article. M.L.R.C. corrected and revised the manuscript according to comments of referees.

Acknowledgments: M.L.R.C. thanks the supporting by the Spanish Ministry of Science and Innovation (CTM2014-56668-R).

Conflicts of Interest: The authors declare no conflict of interest.

References

1. Venkatadri, R.; Peters, R.W. Chemical oxidation technologies: Ultraviolet light/hydrogen peroxide, Fenton's reagent and titanium dioxide-assisted photocatalysis. *Hazard. Waste Hazard. Mater.* **1993**, *10*, 107–149. [CrossRef]
2. Skoumal, M.; Cabot, P.-L.; Centellas, F.; Arias, C.; Rodriguez, R.M.; Garrido, J.A.; Brillas, E. Mineralization of paracetamol by ozonation catalyzed with Fe^{2+}, Cu^{2+} and UVA light. *Appl. Catal. B* **2006**, *66*, 228–240. [CrossRef]
3. Rosenfeldt, E.J.; Chen, P.J.; Kullman, S.; Linden, K.G. Destruction of estrogenic activity in water using UV advanced oxidation. *Sci. Total Environ.* **2007**, *377*, 105–113. [CrossRef] [PubMed]
4. Poyatos, J.M.; Munio, M.M.; Almecija, M.C.; Torres, J.C.; Hontoria, E.; Osorio, F. Advanced oxidation processes for wastewater treatment: State of the art. *Water Air Soil Pollut.* **2010**, *205*, 187–204. [CrossRef]
5. Gogate, P.R.; Pandit, A.B. A review of imperative technologies for wastewater treatment. I: Oxidation technologies at ambient conditions. *Adv. Environ. Res.* **2004**, *8*, 501–551. [CrossRef]
6. Gogate, P.R.; Pandit, A.B. A review of imperative technologies for wastewater treatment. II: Hybrid methods. *Adv. Environ. Res.* **2004**, *8*, 553–597. [CrossRef]
7. Marquez, J.J.R.; Levchuk, I.; Sillanpaa, M. Application of catalytic wet peroxide oxidation for industrial and urban wastewater treatment: A review. *Catalysts* **2018**, *8*, 673/1–673/18.
8. Neyens, E.; Baeyens, J. A review of classic Fenton's peroxidation as an advanced oxidation technique. *J. Hazard. Mater.* **2003**, *98*, 33–50. [CrossRef]
9. Kumar, S.M. Degradation and mineralization of organic contaminants by Fenton and photo-Fenton processes: Review of mechanisms and effects of organic and inorganic additives. *Res. J. Chem. Environ.* **2011**, *15*, 96–112.
10. Oller, I.; Malato, S.; Sanchez-Perez, J.A. Combination of advanced oxidation processes and biological treatments for wastewater decontamination. A review. *Sci. Total Environ.* **2011**, *409*, 4141–4166. [CrossRef] [PubMed]
11. Ferri, D.; Forni, L. Methane combustion on some perovskite-like mixed oxides. *Appl. Catal. B* **1998**, *16*, 119–126. [CrossRef]
12. Zhu, J.; Thomas, A. Perovskite-type mixed oxides as catalytic material for NO removal. *Appl. Catal. B* **2009**, *92*, 225–233. [CrossRef]
13. Tejuca, L.G.; Fierro, J.L.G.; Tascon, J.M.D. Structure and reactivity of perovskite-type oxides. *Adv. Catal.* **1989**, *36*, 237–328.
14. Pena, M.A.; Fierro, J.L.G. Chemical Structures and Performance of Perovskite Oxides. *Chem. Rev.* **2001**, *101*, 1981–2017. [CrossRef] [PubMed]
15. Xu, J.-J.; Xu, D.; Wang, Z.-L.; Wang, H.-G.; Zhang, L.-L.; Zhang, X.-B. Synthesis of perovskite-based porous $La_{0.75}Sr_{0.25}MnO_3$ nanotubes as a highly efficient electrocatalyst for rechargeable lithium-oxygen batteries. *Angew. Chem. Int. Ed* **2013**, *52*, 3887–3890. [CrossRef] [PubMed]
16. Sekhar, P.K.; Mukundan, R.; Brosha, E.; Garzon, F. Effect of perovskite electrode composition on mixed potential sensor response. *Sens. Actuators B* **2013**, *183*, 20–24. [CrossRef]

17. Mori, M.; Itagaki, Y.; Sadaoka, Y. Effect of VOC on ozone detection using semiconducting sensor with $SmFe_{1-x}Co_xO_3$ perovskite-type oxides. *Sens. Actuators B* **2012**, *163*, 44–50. [CrossRef]
18. Tavakkoli, H.; Yazdanbakhsh, M. Fabrication of two perovskite-type oxide nanoparticles as the new adsorbents in efficient removal of a pesticide from aqueous solutions: Kinetic, thermodynamic and adsorption studies. *Microporous Mesoporous Mater.* **2013**, *176*, 86–94. [CrossRef]
19. Royer, S.; Duprez, D.; Can, F.; Courtois, X.; Batiot-Dupeyrat, C.; Laassiri, S.; Alamdari, H. Perovskites as substitutes of noble metals for heterogeneous catalysis: Dream or reality. *Chem. Rev.* **2014**, *114*, 10292–10368. [CrossRef] [PubMed]
20. Soleymani, M.; Moheb, A.; Babakhani, D. Hydrogen peroxide decomposition over nanosized $La_{1-X}Ca_XMnO_3$ ($0 \leq X \leq 0.6$) perovskite oxides. *Chem. Eng. Technol.* **2011**, *34*, 49–55. [CrossRef]
21. Ariafard, A.; Aghabozorg, H.R.; Salehirad, F. Hydrogen peroxide decomposition over $La_{0.9}Sr_{0.1}Ni_{1-x}Cr_xO_3$ perovskites. *Catal. Commun.* **2003**, *4*, 561–566. [CrossRef]
22. Lee, Y.N.; Lago, R.M.; Fierro, J.L.G.; Gonzalez, J. Hydrogen peroxide decomposition over $Ln_{1-x}A_xMnO_3$ (Ln = La or Nd and A = K or Sr) perovskites. *Appl. Catal. A* **2001**, *215*, 245–256. [CrossRef]
23. Garrido-Ramirez, E.G.; Theng, B.K.G.; Mora, M.L. Clays and oxide minerals as catalysts and nanocatalysts in Fenton-like reactions—A review. *Appl. Clay Sci.* **2010**, *47*, 182–192. [CrossRef]
24. Xu, L.; Wang, J. Magnetic nanoscaled Fe_3O_4/CeO_2 composite as an efficient Fenton-Like heterogeneous catalyst for degradation of 4-chlorophenol. *Environ. Sci. Technol.* **2012**, *46*, 10145–10153. [CrossRef] [PubMed]
25. Rahim Pouran, S.; Abdul Raman, A.A.; Wan Daud, W.M.A. Review on the application of modified iron oxides as heterogeneous catalysts in Fenton reactions. *J. Clean. Prod.* **2014**, *64*, 24–35. [CrossRef]
26. Pereira, M.C.; Oliveira, L.C.A.; Murad, E. Iron oxide catalysts: Fenton and Fenton-like reactions—A review. *Clay Miner.* **2012**, *47*, 285–302. [CrossRef]
27. Nidheesh, P.V. Heterogeneous Fenton catalysts for the abatement of organic pollutants from aqueous solution: A review. *RSC Adv.* **2015**, *5*, 40552–40577. [CrossRef]
28. Ramirez, J.H.; Costa, C.A.; Madeira, L.M.; Mata, G.; Vicente, M.A.; Rojas-Cervantes, M.L.; López-Peinado, A.J.; Martín-Aranda, R.M. Fenton-like oxidation of Orange II solutions using heterogeneous catalysts based on saponite clay. *Appl. Catal. B* **2007**, *71*, 44–56. [CrossRef]
29. Navalon, S.; Alvaro, M.; Garcia, H. Heterogeneous Fenton catalysts based on clays, silicas and zeolites. *Appl. Catal. B* **2010**, *99*, 1–26. [CrossRef]
30. Hassan, H.; Hameed, B.H. Iron-clay as effective heterogeneous Fenton catalyst for the decolorization of Reactive Blue 4. *Chem. Eng. J.* **2011**, *171*, 912–918. [CrossRef]
31. Kuznetsova, E.V.; Savinov, E.N.; Vostrikova, L.A.; Parmon, V.N. Heterogeneous catalysis in the Fenton-type system FeZSM-5/H_2O_2. *Appl. Catal. B* **2004**, *51*, 165–170. [CrossRef]
32. Velichkova, F.; Delmas, H.; Julcour, C.; Koumanova, B. Heterogeneous fenton and photo-fenton oxidation for paracetamol removal using iron containing ZSM-5 zeolite as catalyst. *AIChE J.* **2017**, *63*, 669–679. [CrossRef]
33. Ramirez, J.H.; Maldonado-Hodar, F.J.; Perez-Cadenas, A.F.; Moreno-Castilla, C.; Costa, C.A.; Madeira, L.M. Azo-dye Orange II degradation by heterogeneous Fenton-like reaction using carbon-Fe catalysts. *Appl. Catal. B* **2007**, *75*, 312–323. [CrossRef]
34. Duarte, F.; Maldonado-Hodar, F.J.; Perez-Cadenas, A.F.; Madeira, L.M. Fenton-like degradation of azo-dye Orange II catalyzed by transition metals on carbon aerogels. *Appl. Catal. B* **2009**, *85*, 139–147. [CrossRef]
35. Sun, L.; Yao, Y.; Wang, L.; Mao, Y.; Huang, Z.; Yao, D.; Lu, W.; Chen, W. Efficient removal of dyes using activated carbon fibers coupled with 8-hydroxyquinoline ferric as a reusable Fenton-like catalyst. *Chem. Eng. J.* **2014**, *240*, 413–419. [CrossRef]
36. Wang, L.; Yao, Y.; Zhang, Z.; Sun, L.; Lu, W.; Chen, W.; Chen, H. Activated carbon fibers as an excellent partner of Fenton catalyst for dyes decolorization by combination of adsorption and oxidation. *Chem. Eng. J.* **2014**, *251*, 348–354. [CrossRef]
37. Carrasco-Diaz, M.R.; Castillejos-Lopez, E.; Cerpa-Naranjo, A.; Rojas-Cervantes, M.L. On the textural and crystalline properties of Fe-carbon xerogels. Application as Fenton-like catalysts in the oxidation of paracetamol by H_2O_2. *Microporous Mesoporous Mater.* **2017**, *237*, 282–293. [CrossRef]
38. Eberhardt, M.K.; Ramirez, G.; Ayala, E. Does the reaction of copper(I) with hydrogen peroxide give hydroxyl radicals? A study of aromatic hydroxylation. *J. Org. Chem.* **1989**, *54*, 5922–5926. [CrossRef]

39. Lassmann, G.; Eriksson, L.A.; Himo, F.; Lendzian, F.; Lubitz, W. Electronic Structure of a Transient Histidine Radical in Liquid Aqueous Solution: EPR Continuous-Flow Studies and Density Functional Calculations. *J. Phys. Chem. A* **1999**, *103*, 1283–1290. [CrossRef]
40. Li, H.; Wan, J.; Ma, Y.; Wang, Y.; Chen, X.; Guan, Z. Degradation of refractory dibutyl phthalate by peroxymonosulfate activated with novel catalysts cobalt metal-organic frameworks: Mechanism, performance and stability. *J. Hazard. Mater.* **2016**, *318*, 154–163. [CrossRef] [PubMed]
41. Rivas, F.J.; Carbajo, M.; Beltran, F.J.; Acedo, B.; Gimeno, O. Perovskite catalytic ozonation of pyruvic acid in water. *Appl. Catal. B* **2006**, *62*, 93–103. [CrossRef]
42. Carbajo, M.; Rivas, F.J.; Beltran, F.J.; Alvarez, P.; Medina, F. Effects of different catalysts on the ozonation of pyruvic acid in water. *Ozone Sci. Eng.* **2006**, *28*, 229–235. [CrossRef]
43. Carbajo, M.; Beltran, F.J.; Medina, F.; Gimeno, O.; Rivas, F.J. Catalytic ozonation of phenolic compounds. *Appl. Catal. B* **2006**, *67*, 177–186. [CrossRef]
44. Carbajo, M.; Beltran, F.J.; Gimeno, O.; Acedo, B.; Rivas, F.J. Ozonation of phenolic wastewaters in the presence of a perovskite type catalyst. *Appl. Catal. B* **2007**, *74*, 203–210. [CrossRef]
45. Beltran, F.J.; Pocostales, P.; Alvarez, P.M.; Lopez-Pineiro, F. Catalysts to improve the abatement of sulfamethoxazole and the resulting organic carbon in water during ozonation. *Appl. Catal. B* **2009**, *92*, 262–270. [CrossRef]
46. Beltran, F.J.; Pocostales, P.; Alvarez, P.; Garcia-Araya, J.F.; Gimeno, O. Perovskite catalytic ozonation of some pharmaceutical compounds in water. *Ozone Sci. Eng.* **2010**, *32*, 230–237. [CrossRef]
47. Orge, C.A.; Orfao, J.J.M.; Pereira, M.F.R.; Barbero, B.P.; Cadus, L.E. Lanthanum-based perovskites as catalysts for the ozonation of selected organic compounds. *Appl. Catal. B* **2013**, *140-141*, 426–432. [CrossRef]
48. Afzal, S.; Quan, X.; Zhang, J. High surface area mesoporous nanocast $LaMO_3$ (M = Mn, Fe) perovskites for efficient catalytic ozonation and an insight into probable catalytic mechanism. *Appl. Catal. B* **2017**, *206*, 692–703. [CrossRef]
49. Zhang, Y.; Xia, Y.; Li, Q.; Qi, F.; Xu, B.; Chen, Z. Synchronously degradation benzotriazole and elimination bromate by perovskite oxides catalytic ozonation: Performance and reaction mechanism. *Sep. Purif. Technol.* **2018**, *197*, 261–270. [CrossRef]
50. Beltran, F.J.; Aguinaco, A.; Garcia-Araya, J.F.; Oropesa, A.L. Ozone and photocatalytic processes to remove the antibiotic sulfamethoxazole from water. *Water Res.* **2008**, *42*, 3799–3808. [CrossRef] [PubMed]
51. Rivas, F.J.; Carbajo, M.; Beltran, F.; Gimeno, O.; Frades, J. Comparison of different advanced oxidation processes (AOPs) in the presence of perovskites. *J. Hazard. Mater.* **2008**, *155*, 407–414. [CrossRef] [PubMed]
52. De Laat, J.; Gallard, H. Catalytic Decomposition of hydrogen peroxide by Fe(III) in homogeneous aqueous solution: Mechanism and kinetic modeling. *Environ. Sci. Technol.* **1999**, *33*, 2726–2732. [CrossRef]
53. Bokare, A.D.; Choi, W. Review of iron-free Fenton-like systems for activating H_2O_2 in advanced oxidation processes. *J. Hazard. Mater.* **2014**, *275*, 121–135. [CrossRef] [PubMed]
54. Luo, W.; Zhu, L.; Wang, N.; Tang, H.; Cao, M.; She, Y. Efficient removal of organic pollutants with magnetic nanoscaled $BiFeO_3$ as a reusable heterogeneous Fenton-like catalyst. *Environ. Sci. Technol.* **2010**, *44*, 1786–1791. [CrossRef] [PubMed]
55. Zhang, L.; Nie, Y.; Hu, C.; Qu, J. Enhanced Fenton degradation of Rhodamine B over nanoscaled Cu-doped $LaTiO_3$ perovskite. *Appl. Catal. B* **2012**, *125*, 418–424. [CrossRef]
56. Xiao, P.; Hong, J.; Wang, T.; Xu, X.; Yuan, Y.; Li, J.; Zhu, J. Oxidative degradation of organic dyes over supported perovskite oxide $LaFeO_3$/SBA-15 under ambient conditions. *Catal. Lett.* **2013**, *143*, 887–894. [CrossRef]
57. Xiao, P.; Li, H.; Wang, T.; Zhu, J. Efficient Fenton-like La-Cu-O/SBA-15 catalyst for the degradation of organic dyes under ambient conditions. *RSC Adv.* **2014**, *4*, 12601–12604. [CrossRef]
58. Li, H.; Zhu, J.; Xiao, P.; Zhan, Y.; Lv, K.; Wu, L.; Li, M. On the mechanism of oxidative degradation of rhodamine B over $LaFeO_3$ catalysts supported on silica materials: Role of support. *Microporous Mesoporous Mater.* **2016**, *221*, 159–166. [CrossRef]
59. Giuseppina Iervolinoa, V.V.; Sanninoa, D.; Rizzob, L.; Sarnoa, G.; Lyubov, P.C.; Isupovac, A. Influence of operating conditions in the photo-Fenton removal of tartrazine on structured catalysts. *Chem. Eng. Trans.* **2015**, *43*, 979–984.
60. Zhao, H.; Cao, J.; Lv, H.; Wang, Y.; Zhao, G. 3D nano-scale perovskite-based composite as Fenton-like system for efficient oxidative degradation of ketoprofen. *Catal. Commun.* **2013**, *41*, 87–90. [CrossRef]

61. Li, J.; Miao, J.; Duan, X.; Dai, J.; Liu, Q.; Wang, S.; Zhou, W.; Shao, Z. Fine-tuning surface properties of perovskites via nanocompositing with inert oxide toward ceveloping superior catalysts for advanced oxidation. *Adv. Funct. Mater.* **2018**, *28*, 1804654. [CrossRef]
62. Nie, Y.; Zhang, L.; Li, Y.-Y.; Hu, C. Enhanced Fenton-like degradation of refractory organic compounds by surface complex formation of $LaFeO_3$ and H_2O_2. *J. Hazard. Mater.* **2015**, *294*, 195–200. [CrossRef] [PubMed]
63. Rusevova, K.; Koeferstein, R.; Rosell, M.; Richnow, H.H.; Kopinke, F.-D.; Georgi, A. $LaFeO_3$ and $BiFeO_3$ perovskites as nanocatalysts for contaminant degradation in heterogeneous Fenton-like reactions. *Chem. Eng. J.* **2014**, *239*, 322–331. [CrossRef]
64. Taran, O.P.; Ayusheev, A.B.; Ogorodnikova, O.L.; Prosvirin, I.P.; Isupova, L.A.; Parmon, V.N. Perovskite-like catalysts $LaBO_3$ (B = Cu, Fe, Mn, Co, Ni) for wet peroxide oxidation of phenol. *Appl. Catal. B* **2016**, *180*, 86–93. [CrossRef]
65. Ben Hammouda, S.; Zhao, F.; Safaei, Z.; Babu, I.; Ramasamy, D.L.; Sillanpaa, M. Reactivity of Ceria-Perovskite composites CeO_2-$LaMO_3$ (M=Cu, Fe) in catalytic wet peroxidative oxidation of pollutant Bisphenol F: Characterization, kinetic and mechanism studies. *Appl. Catal. B* **2017**, *218*, 119–136. [CrossRef]
66. Wang, N.; Zhu, L.; Lei, M.; She, Y.; Cao, M.; Tang, H. Ligand-induced drastic enhancement of catalytic activity of nano-$BiFeO_3$ for oxidative degradation of bisphenol A. *ACS Catal.* **2011**, *1*, 1193–1202. [CrossRef]
67. Song, Z.; Wang, N.; Zhu, L.; Huang, A.; Zhao, X.; Tang, H. Efficient oxidative degradation of triclosan by using an enhanced Fenton-like process. *Chem. Eng. J.* **2012**, *198-199*, 379–387. [CrossRef]
68. Magalhaes, F.; Moura, F.C.C.; Ardisson, J.D.; Lago, R.M. $LaMn_{1-x}Fe_xO_3$ and $LaMn_{0.1-x}Fe_{0.90}Mo_xO_3$ perovskites: Synthesis, characterization and catalytic activity in H_2O_2 reactions. *Mater. Res.* **2008**, *11*, 307–312. [CrossRef]
69. Jauhar, S.; Dhiman, M.; Bansal, S.; Singhal, S. Mn^{3+} ion in perovskite lattice: A potential Fenton's reagent exhibiting remarkably enhanced degradation of cationic and anionic dyes. *J. Sol-Gel Sci. Technol.* **2015**, *75*, 124–133. [CrossRef]
70. Carrasco-Diaz, M.R.; Castillejos-Lopez, E.; Cerpa-Naranjo, A.; Rojas-Cervantes, M.L. Efficient removal of paracetamol using $LaCu_{1-x}M_xO_3$ (M = Mn, Ti) perovskites as heterogeneous Fenton-like catalysts. *Chem. Eng. J.* **2016**, *304*, 408–418. [CrossRef]
71. Sannino, D.; Vaiano, V.; Ciambelli, P.; Isupova, L.A. Mathematical modelling of the heterogeneous photo-Fenton oxidation of acetic acid on structured catalysts. *Chem. Eng. J.* **2013**, *224*, 53–58. [CrossRef]
72. Loghambal, S.; Agvinos Catherine, A.J. Mathematical analysis of the heterogeneous photo-Fenton oxidation of acetic acid on structured catalysts. *J. Math. Chem.* **2016**, *54*, 1146–1158. [CrossRef]
73. Singh, C.; Rakesh, M. Oxidation of phenol using $LaMnO_3$ perovskite, TiO_2, H_2O_2 and UV radiation. *Indian J. Chem. Technol.* **2010**, *17*, 451–454.
74. Soltani, T.; Lee, B.-K. Enhanced formation of sulfate radicals by metal-doped $BiFeO_3$ under visible light for improving photo-Fenton catalytic degradation of 2-chlorophenol. *Chem. Eng. J.* **2017**, *313*, 1258–1268. [CrossRef]
75. Ju, L.; Chen, Z.; Fang, L.; Dong, W.; Zheng, F.; Shen, M. Sol-gel synthesis and photo-Fenton-like catalytic activity of $EuFeO_3$ nanoparticles. *J. Am. Ceram. Soc.* **2011**, *94*, 3418–3424. [CrossRef]
76. Phan, T.T.N.; Nikoloski, A.N.; Bahri, P.A.; Li, D. Heterogeneous photo-Fenton degradation of organics using highly efficient Cu-doped $LaFeO_3$ under visible light. *J. Ind. Eng. Chem.* **2018**, *61*, 53–64. [CrossRef]
77. Sannino, D.; Vaiano, V.; Ciambelli, P.; Isupova, L.A. Structured catalysts for photo-Fenton oxidation of acetic acid. *Catal. Today* **2011**, *161*, 255–259. [CrossRef]
78. Sannino, D.; Vaiano, V.; Isupova, L.A.; Ciambelli, P. Heterogeneous photo-Fenton oxidation of organic pollutants on structured catalysts. *J. Adv. Oxid. Technol.* **2012**, *15*, 294–300. [CrossRef]
79. Vaiano, V.; Isupova, L.A.; Ciambelli, P.; Sannino, D. Photo-fenton oxidation of t-butyl methyl ether in presence of $LaFeO_3$ supported on monolithic structure. *J. Adv. Oxid. Technol.* **2014**, *17*, 187–192. [CrossRef]
80. Orak, C.; Atalay, S.; Ersoz, G. Photocatalytic and photo-Fenton-like degradation of methylparaben on monolith-supported perovskite-type catalysts. *Sep. Sci. Technol.* **2017**, *52*, 1310–1320. [CrossRef]
81. An, J.; Zhu, L.; Wang, N.; Song, Z.; Yang, Z.; Du, D.; Tang, H. Photo-Fenton like degradation of tetrabromobisphenol A with graphene $BiFeO_3$ composite as a catalyst. *Chem. Eng. J.* **2013**, *219*, 225–237. [CrossRef]

82. Kondrakov, A.O.; Ignatev, A.N.; Lunin, V.V.; Frimmel, F.H.; Braese, S.; Horn, H. Roles of water and dissolved oxygen in photocatalytic generation of free OH radicals in aqueous TiO_2 suspensions: An isotope labeling study. *Appl. Catal. B* **2016**, *182*, 424–430. [CrossRef]
83. Chiou, C.-S.; Chen, Y.-H.; Chang, C.-T.; Chang, C.-Y.; Shie, J.-L.; Li, Y.-S. Photochemical mineralization of di-n-butyl phthalate with H_2O_2/Fe^{3+}. *J. Hazard. Mater.* **2006**, *135*, 344–349. [CrossRef] [PubMed]
84. Li, X.; Liu, Y.; Wang, C.; Yin, K. Study of the stability of H_2O_2 in alkaline slurry. *Bandaoti Jishu* **2012**, *37*, 850–854.
85. Ovejero, G.; Sotelo, J.L.; Martinez, F.; Gordo, L. Novel heterogeneous catalysts in the wet peroxide oxidation of phenol. *Water Sci. Technol.* **2001**, *44*, 153–160. [CrossRef] [PubMed]
86. Sotelo, J.L.; Ovejero, G.; Martinez, F.; Melero, J.A.; Milieni, A. Catalytic wet peroxide oxidation of phenolic solutions over a $LaTi_{1-x}Cu_xO_3$ perovskite catalyst. *Appl. Catal. B* **2004**, *47*, 281–294. [CrossRef]
87. Faye, J.; Guelou, E.; Barrault, J.; Tatibouet, J.M.; Valange, S. $LaFeO_3$ Perovskite as new and performant catalyst for the wet peroxide oxidation of organic pollutants in ambient conditions. *Top. Catal.* **2009**, *52*, 1211–1219. [CrossRef]
88. Guerra-Rodríguez, S.; Rodríguez, E.; Singh, N.D.; Rodríguez-Chueca, J. Assessment of Sulfate Radical-Based Advanced Oxidation Processes for Water and Wastewater Treatment: A Review. *Water* **2018**, *10*, 1828. [CrossRef]
89. Ghanbari, F.; Moradi, M. Application of peroxymonosulfate and its activation methods for degradation of environmental organic pollutants: Review. *Chem. Eng. J.* **2017**, *310*, 41–62. [CrossRef]
90. Khan, A.; Liao, Z.; Liu, Y.; Jawad, A.; Ifthikar, J.; Chen, Z. Synergistic degradation of phenols using peroxymonosulfate activated by $CuO\text{-}Co_3O_4@MnO_2$ nanocatalyst. *J. Hazard. Mater.* **2017**, *329*, 262–271. [CrossRef] [PubMed]
91. Duan, X.; Ao, Z.; Sun, H.; Indrawirawan, S.; Wang, Y.; Kang, J.; . Liang, F.; Zhu, Z.H.; Wang, S. Nitrogen-doped graphene for generation and evolution of reactive radicals by metal-free catalysis. *ACS Appl. Mater. Interfaces* **2015**, *7*, 4169–4178. [CrossRef] [PubMed]
92. Anipsitakis, G.P.; Dionysiou, D.D.; Gonzalez, M.A. Cobalt-mediated activation of peroxymonosulfate and sulfate radical attack on phenolic compounds. Implications of chloride ions. *Environ. Sci. Technol.* **2006**, *40*, 1000–1007. [CrossRef] [PubMed]
93. Sun, H.; Liang, H.; Zhou, G.; Wang, S. Supported cobalt catalysts by one-pot aqueous combustion synthesis for catalytic phenol degradation. *J. Colloid Interface Sci.* **2013**, *394*, 394–400. [CrossRef] [PubMed]
94. Ji, Y.; Dong, C.; Kong, D.; Lu, J. New insights into atrazine degradation by cobalt catalyzed peroxymonosulfate oxidation: Kinetics, reaction products and transformation mechanisms. *J. Hazard. Mater.* **2015**, *285*, 491–500. [CrossRef] [PubMed]
95. Ben Hammouda, S.; Zhao, F.; Safaei, Z.; Srivastava, V.; Lakshmi Ramasamy, D.; Iftekhar, S.; . kalliola, S.; Sillanpää, M. Degradation and mineralization of phenol in aqueous medium by heterogeneous monopersulfate activation on nanostructured cobalt based-perovskite catalysts $ACoO_3$ (A = La, Ba, Sr and Ce): Characterization, kinetics and mechanism study. *Appl. Catal. B* **2017**, *215*, 60–73. [CrossRef]
96. Su, C.; Duan, X.; Miao, J.; Zhong, Y.; Zhou, W.; Wang, S.; Shao, Z. Mixed conducting perovskite materials as superior catalysts for fast aqueous-phase advanced oxidation: A mechanistic study. *ACS Catal.* **2017**, *7*, 388–397. [CrossRef]
97. Lin, K.-Y.A.; Chen, Y.-C.; Lin, T.-Y.; Yang, H. Lanthanum cobaltite perovskite supported on zirconia as an efficient heterogeneous catalyst for activating Oxone in water. *J. Colloid Interface Sci.* **2017**, *497*, 325–332. [CrossRef] [PubMed]
98. Miao, J.; Zhou, W.; Shao, Z.; Sunarso, J.; Su, C.; Wang, S. $SrCo_{1-x}TixO_{3-\delta}$ perovskites as excellent catalysts for fast degradation of water contaminants in neutral and alkaline solutions. *Sci. Rep.* **2017**, *7*, 44215. [CrossRef] [PubMed]
99. Duan, X.; Su, C.; Miao, J.; Zhong, Y.; Shao, Z.; Wang, S. Sun, H. Insights into perovskite-catalyzed peroxymonosulfate activation: Maneuverable cobalt sites for promoted evolution of sulfate radicals. *Appl. Catal. B* **2018**, *220*, 626–634. [CrossRef]
100. Lu, S.; Wang, G.; Chen, S.; Yu, H.; Ye, F.; Quan, X. Heterogeneous activation of peroxymonosulfate by $LaCo_{1-x}Cu_xO_3$ perovskites for degradation of organic pollutants. *J. Hazard. Mater.* **2018**, *353*, 401–409. [CrossRef] [PubMed]

101. Miao, J.; Sunarso, J.; Duan, X.; Zhou, W.; Wang, S.; Shao, Z. Nanostructured Co-Mn containing perovskites for degradation of pollutants: Insight into the activity and stability. *J. Hazard. Mater.* **2018**, *349*, 177–185. [CrossRef] [PubMed]
102. Pang, X.; Guo, Y.; Zhang, Y.; Xu, B.; Qi, F. $LaCoO_3$ perovskite oxide activation of peroxymonosulfate for aqueous 2-phenyl-5-sulfobenzimidazole degradation: Effect of synthetic method and the reaction mechanism. *Chem. Eng. J.* **2016**, *304*, 897–907. [CrossRef]
103. RSolis, R.; Rivas, F.J.; Gimeno, O. Removal of aqueous metazachlor, tembotrione, tritosulfuron and ethofumesate by heterogeneous monopersulfate decomposition on lanthanum-cobalt perovskites. *Appl. Catal. B* **2017**, *200*, 83–92. [CrossRef]
104. Lin, K.-Y.A.; Chen, Y.-C.; Lin, Y.-F. $LaMO_3$ perovskites (M=Co, Cu, Fe and Ni) as heterogeneous catalysts for activating peroxymonosulfate in water. *Chem. Eng. Sci.* **2017**, *160*, 96–105. [CrossRef]
105. Rao, Y.; Zhang, Y.; Han, F.; Guo, H.; Huang, Y.; Li, R.; Qi, F.; Ma, J. Heterogeneous activation of peroxymonosulfate by $LaFeO_3$ for diclofenac degradation: DFT-assisted mechanistic study and degradation pathways. *Chem. Eng. J.* **2018**, *352*, 601–611. [CrossRef]
106. Chu, Y.; Tan, X.; Shen, Z.; Liu, P.; Han, N.; Kang, J.; Duan, X.; Wang, S.; Liu, L.; Liu, S. Efficient removal of organic and bacterial pollutants by Ag-$La_{0.8}Ca_{0.2}Fe_{0.94}O_{3-\delta}$ perovskite via catalytic peroxymonosulfate activation. *J. Hazard. Mater.* **2018**, *356*, 53–60. [CrossRef] [PubMed]
107. Chi, F.; Song, B.; Yang, B.; Lv, Y.; Ran, S.; Huo, Q. Activation of peroxymonosulfate by $BiFeO_3$ microspheres under visible light irradiation for decomposition of organic pollutants. *RSC Adv.* **2015**, *5*, 67412–67417. [CrossRef]
108. Solis, R.R.; Rivas, F.J.; Gimeno, O.; Perez-Bote, J.-L. Synergism between peroxymonosulfate and $LaCoO_3$-TiO_2 photocatalysis for oxidation of herbicides. Operational variables and catalyst characterization assessment. *J. Chem. Technol. Biotechnol.* **2017**, *92*, 2159–2170. [CrossRef]
109. Ben Hammouda, S.; Zhao, F.; Safaei, Z.; Ramasamy, D.L.; Doshi, B.; Sillanpaa, M. Sulfate radical-mediated degradation and mineralization of bisphenol F in neutral medium by the novel magnetic Sr_2CoFeO_6 double perovskite oxide catalyzed peroxymonosulfate: Influence of co-existing chemicals and UV irradiation. *Appl. Catal. B* **2018**, *233*, 99–111. [CrossRef]
110. Fendrich, A.M.; Quaranta, A.; Orlandi, M.; Bettonte, M.; Miotello, A. Solar Concentration for Wastewaters Remediation: A Review of Materials and Technologies. *Appl. Sci.* **2018**, *9*, 118. [CrossRef]
111. Li, S.; Jing, L.; Fu, W.; Yang, L.; Xin, B.; Fu, H. Photoinduced charge property of nanosized perovskite-type $LaFeO_3$ and its relationships with photocatalytic activity under visible irradiation. *Mater. Res. Bull.* **2007**, *42*, 203–212. [CrossRef]
112. Su, H.J.; Jing, L.Q.; Shi, K.Y.; Yao, C.H.; Fu, H.G. Synthesis of large surface area $LaFeO_3$ nanoparticles by SBA-16 template method as high active visible photocatalysts. *J. Nanopart. Res.* **2010**, *12*, 967–974. [CrossRef]
113. Hu, R.; Li, C.; Wang, X.; Sun, Y.; Jia, H.; Su, H.; Zhang, Y. Photocatalytic activities of $LaFeO_3$ and La_2FeTiO_6 in p-chlorophenol degradation under visible light. *Catal. Commun.* **2012**, *29*, 35–39. [CrossRef]
114. Li, L.; Wang, X.; Zhang, Y. Enhanced visible light-responsive photocatalytic activity of $LnFeO_3$ (Ln = La, Sm) nanoparticles by synergistic catalysis. *Mater. Res. Bull.* **2014**, *50*, 18–22. [CrossRef]
115. Hou, L.; Sun, G.; Liu, K.; Li, Y.; Gao, F. Preparation, characterization and investigation of catalytic activity of Li-doped $LaFeO_3$ nanoparticles. *J. Sol-Gel Sci. Technol.* **2006**, *40*, 9–14. [CrossRef]
116. Shen, H.; Xue, T.; Wang, Y.; Cao, G.; Lu, Y.; Fang, G. Photocatalytic property of perovskite $LaFeO_3$ synthesized by sol-gel process and vacuum microwave calcination. *Mater. Res. Bull.* **2016**, *84*, 15–24. [CrossRef]
117. Tang, P.; Tong, Y.; Chen, H.; Cao, F.; Pan, G. Microwave-assisted synthesis of nanoparticulate perovskite $LaFeO_3$ as a high active visible-light photocatalyst. *Curr. Appl. Phys.* **2013**, *13*, 340–343. [CrossRef]
118. Li, F.-t.; Liu, Y.; Liu, R.-h.; Sun, Z.-m.; Zhao, D.-s.; Kou, C.-g. Preparation of Ca-doped $LaFeO_3$ nanopowders in a reverse microemulsion and their visible light photocatalytic activity. *Mater. Lett.* **2010**, *64*, 223–225. [CrossRef]
119. Thirumalairajan, S.; Girija, K.; Ganesh, I.; Mangalaraj, D.; Viswanathan, C.; Balamurugan, A.; Ponpandian, N. Controlled synthesis of perovskite LaFeO3 microsphere composed of nanoparticles via self-assembly process and associated photocatalytic activity. *Chem. Eng. J.* **2012**, *209*, 420–428. [CrossRef]
120. Ding, J.; Lue, X.; Shu, H.; Xie, J.; Zhang, H. Microwave-assisted synthesis of perovskite $ReFeO_3$ (Re: La, Sm, Eu, Gd) photocatalyst. *Mater. Sci. Eng. B* **2010**, *171*, 31–34. [CrossRef]

121. Liang, Q.; Jin, J.; Liu, C.; Xu, S.; Li, Z. Constructing a novel p-n heterojunction photocatalyst $LaFeO_3$/g-C_3N_4 with enhanced visible-light-driven photocatalytic activity. *J. Alloy. Compd.* **2017**, *709*, 542–548. [CrossRef]
122. Ren, X.; Yang, H.; Sai, G.; Zhou, J.; Yang, T.; Zhang, X.; Cheng, Z.; Sun, S. Controlled growth of $LaFeO_3$ nanoparticles on reduced graphene oxide for highly efficient photocatalysis. *Nanoscale* **2016**, *8*, 752–756. [CrossRef] [PubMed]
123. Fu, S.; Niu, H.; Tao, Z.; Song, J.; Mao, C.; Zhang, S.; Chen, C.; Wang, D. Low temperature synthesis and photocatalytic property of perovskite-type $LaCoO_3$ hollow spheres. *J. Alloys Compd.* **2013**, *576*, 5–12. [CrossRef]
124. Song, S.; Xu, L.; He, Z.; Chen, J.; Xiao, X.; Yan, B. Mechanism of the Photocatalytic Degradation of C.I. Reactive Black 5 at pH 12.0 Using $SrTiO_3$/CeO_2 as the Catalyst. *Environ. Sci. Technol.* **2007**, *41*, 5846–5853. [CrossRef] [PubMed]
125. Song, S.; Xu, L.J.; He, Z.Q.; Ying, H.P.; Chen, J.M.; Xiao, X.Z.; Yan, B. Photocatalytic degradation of CI Direct Red 23 in aqueous solutions under UV irradiation using $SrTiO_3$/CeO_2 composite as the catalyst. *J. Hazard. Mater.* **2008**, *152*, 1301–1308. [CrossRef] [PubMed]
126. Huerta-Flores, A.M.; Sanchez-Martinez, D.; del Rocio Hernandez-Romero, M.; Zarazua-Morin, M.E.; Torres-Martinez, L.M. Visible-light-driven $BaBiO_3$ perovskite photocatalysts: Effect of physicochemical properties on the photoactivity towards water splitting and the removal of rhodamine B from aqueous systems. *J. Photochem. Photobiol. A* **2019**, *368*, 70–77. [CrossRef]
127. Zheng, H.X.; Zhang, T.T.; Zhu, Y.M.; Liang, B.; Jiang, W. $KBiO_3$ as an Effective Visible-Light-Driven Photocatalyst: Degradation Mechanism for Different Organic Pollutants. *Chemphotochem* **2018**, *2*, 442–449. [CrossRef]
128. Sun, S.; Wang, W.; Zhang, L.; Shang, M. Visible Light-Induced Photocatalytic Oxidation of Phenol and Aqueous Ammonia in Flowerlike $Bi_2Fe_4O_9$ Suspensions. *J. Phys. Chem. C* **2009**, *113*, 12826–12831. [CrossRef]
129. Gao, F.; Chen, X.; Yin, K.; Dong, S.; Ren, Z.; Yuan, F.; Yu, T.; Zou, Z.G.; Liu, J.-M. Visible-light photocatalytic properties of weak magnetic $BiFeO_3$ nanoparticles. *Adv. Mater.* **2007**, *19*, 2889–2892. [CrossRef]
130. Huang, H.; Lu, B.; Liu, Y.; Wang, X.; Hu, J. Synthesis of $LaMnO_3$-Diamond Composites and Their Photocatalytic Activity in the Degradation of Weak Acid Red C-3GN. *Nano* **2018**, *13*, 1850121. [CrossRef]
131. Chasse, M.; Hallett-Tapley, G.L. Gold nanoparticle-functionalized niobium oxide perovskites as photocatalysts for visible light-induced aromatic alcohol oxidations. *Can. J. Chem.* **2018**, *96*, 664–671. [CrossRef]
132. Ohno, T.; Tsubota, T.; Nakamura, Y.; Sayama, K. Preparation of S, C cation-codoped $SrTiO_3$ and its photocatalytic activity under visible light. *Appl. Catal. A-Gen.* **2005**, *288*, 74–79. [CrossRef]
133. Dong, B.; Li, Z.C.; Li, Z.Y.; Xu, X.R.; Song, M.X.; Zheng, W.; Wang, C.; Al-Deyab, S.S.; El-Newehy, M. Highly Efficient $LaCoO_3$ Nanofibers Catalysts for Photocatalytic Degradation of Rhodamine, B. *J. Am. Ceram. Soc.* **2010**, *93*, 3587–3590. [CrossRef]
134. Qin, C.; Li, Z.; Chen, G.; Zhao, Y.; Lin, T. Fabrication and visible-light photocatalytic behavior of perovskite praseodymium ferrite porous nanotubes. *J. Power Sources* **2015**, *285*, 178–184. [CrossRef]
135. Xiang, Q.; Lang, D.; Shen, T.; Liu, F. Graphene-modified nanosized Ag_3PO_4 photocatalysts for enhanced visible-light photocatalytic activity and stability. *Appl. Catal. B* **2015**, *162*, 196–203. [CrossRef]
136. Guo, J.; Dai, Y.-z.; Chen, X.-j.; Zhou, L.-l.; Liu, T.-h. Synthesis and characterization of Ag_3PO_4/$LaCoO_3$ nanocomposite with superior mineralization potential for bisphenol A degradation under visible light. *J. Alloys Compd.* **2017**, *696*, 226–233. [CrossRef]
137. Gao, K.; Li, S. Multi-modal TiO_2–$LaFeO_3$ composite films with high photocatalytic activity and hydrophilicity. *Appl. Surf. Sci.* **2012**, *258*, 6460–6464. [CrossRef]
138. Dhinesh Kumar, R.; Thangappan, R.; Jayavel, R. Synthesis and characterization of $LaFeO_3$/TiO_2 nanocomposites for visible light photocatalytic activity. *J. Phys. Chem. Solids* **2017**, *101*, 25–33. [CrossRef]
139. Schunemann, S.; van Gastel, M.; Tuysuz, H.A. $CsPbBr_3$/TiO_2 Composite for Visible-Light-Driven Photocatalytic Benzyl Alcohol Oxidation. *Chemsuschem* **2018**, *11*, 2057–2061. [CrossRef] [PubMed]
140. Li, G.; Zhang, Y.; Wu, L.; Wu, F.; Wang, R.; Zhang, D.; Zhu, J.; Li, H. An efficient round-the-clock La_2NiO_4 catalyst for breaking down phenolic pollutants. *RSC Adv.* **2012**, *2*, 4822–4828. [CrossRef]
141. Sun, M.; Jiang, Y.; Li, F.; Xia, M.; Xue, B.; Liu, D. Dye degradation activity and stability of perovskite-type $LaCoO_{3-x}$ (x = 0∼0.075). *Mater. Trans.* **2010**, *51*, 2208–2214. [CrossRef]

142. Tummino, M.L.; Laurenti, E.; Deganello, F.; Bianco Prevot, A.; Magnacca, G. Revisiting the catalytic activity of a doped $SrFeO_3$ for water pollutants removal: Effect of light and temperature. *Appl. Catal. B* **2017**, *207*, 174–181. [CrossRef]
143. Wu, J.-M.; Wen, W. Catalyzed degradation of azo dyes under ambient conditions. *Environ. Sci. Technol.* **2010**, *44*, 9123–9127. [CrossRef] [PubMed]
144. Zhong, W.; Jiang, T.; Dang, Y.; He, J.; Chen, S.-Y.; Kuo, C.-H.; Kriz, D.; Meng, Y.; Meguerdichian, A.G.; Suib, S.T. Mechanism studies on Methyl Orange dye degradation by perovskite-type $LaNiO_{3-\delta}$ under dark ambient conditions. *Appl. Catal. A* **2018**, *549*, 302–3099. [CrossRef]
145. Leiw, M.Y.; Guai, G.H.; Wang, X.; Tse, M.S.; Ng, C.M.; Tan, O.K. Dark ambient degradation of Bisphenol A and Acid Orange 8 as organic pollutants by perovskite $SrFeO_{3-\delta}$ metal oxide. *J. Hazard. Mater.* **2013**, *260*, 1–8. [CrossRef] [PubMed]
146. Chen, H.; Motuzas, J.; Martens, W.; Diniz da Costa, J.C. Degradation of azo dye Orange II under dark ambient conditions by calcium strontium copper perovskite. *Appl. Catal. B* **2018**, *221*, 691–700. [CrossRef]